Post-Print version

https://link.springer.com/article/10.1007/s11356-018-2237-2

https://doi.org/10.1007/s11356-018-2237-2

Environmental Science and Pollution Research, 25, June 2018, Pages 23929-23945

Carbonaceous PM10 and PM2.5 and secondary organic aerosol in a coastal rural site near Brindisi (Southern Italy)

Tiziana Siciliano[a], Maria Siciliano[b], Cosimino Malitesta[b], Antonio Proto[c], Raffaele Cucciniello[c], Aldo Giove[d], Silvana Iacobellis[e], Alessandra Genga[b]

[a]Dipartimento Beni Culturali, Università del Salento, Lecce, Puglia, 73100, Italy
[b]Dipartimento di Scienze e Tecnologie Biologiche ed Ambientali, Università del Salento, Lecce, Puglia, 73100, Italy
[c]Department of Chemistry and Biology, University of Salerno, via Giovanni Paolo II, 132 – 84084 – Fisciano (SA), Italy
[d]Generation Italy - Technical Support ENEL, c/o Centrale Federico II, Litoranea Salentina Brindisi-Casalabate – Località Cerano - 72020 Tuturano (Brindisi) - Italia
[e]Italy Health, Safety, Environment & Quality Generation Italy ENEL, Via Arno 44, 00198 ROMA - Italia

***Corresponding author:**
Genga Alessandra
tel +390832297074
e.mail: alessandra.genga@unisalento.it

graphical abstract

Highlights

- Organic carbon and elemental carbon exhibited higher concentrations during the night hours.
- The highest values of OC and EC, OC_{sec} and OC_{prim} were measured when the air masses were coming from Northeastern Europe.
- In dusty days OC_{sec} and OC_{prim} values are slightly higher than in dust free days.
- When the air masses come from Northeastern Europe, OC is mainly characterized by aliphatic and aromatic C-H and O-H and N-H groups.
- Organonitrate, aromatic amide and amine and carboxylic acids are mainly present in samples of air masses coming from Northeastern Europe.
- Kaolinite and carbonate are mainly present in coarse dusty samples.

Abstract

Organic and elemental carbon were measured both in daily PM10 and PM2.5 and in 6 hour range time PM2.5 samples collected from September 2015 to October 2015 in a coastal rural site near Brindisi in the Apulia region (Italy), in order to determine factors affecting the carbonaceous aerosol variations.

Carbon content (total carbon TC) represented a considerable fraction for both PM10 and PM2.5. In particular, in PM10 samples, OC varied from 1.06 to 18.32 μg m^{-3} with a mean concentration of 5 ± 4 μg m^{-3} and EC varied from 0.11 to 0.88 μg m^{-3} with a mean value of 0.41 ± 0.19 μg m^{-3}. In PM2.5 samples, OC varied from 0.54 to 12.91 μg m^{-3} with a mean concentration of 3.5 ± 2.8 μg m^{-3} and EC varied from 0.11 to 0.85 μg m^{-3} with a mean value of 0.35 ± 0.18 μg m^{-3}. The highest values for both parameters were recorded when the air masses were coming from NE Europe and when Saharan Dust events were recognized. The results show that OC and EC exhibited higher concentrations during the night hours, suggesting that stable atmosphere and lower mixing conditions play important roles for the accumulation of air pollutants and promote condensation or adsorption of semivolatile organic compounds.

In samples from a Saharan Dust event and in samples with the lowest and the highest OC_{sec}, ATR-FTIR analysis allowed us to identify organic functional groups including the non-acid organic hydroxyl C-OH group (eg sugars, anhydrosugars, and polyols), carbonyl C=O group, carboxylic acid COOH group, aromatic and aliphatic unsaturated C=C-H group, aliphatic saturated C-C-H group, and amine NH2 group. Some inorganic ions were also identified: carbonates, sulfate, silicate and ammonium. The dusty samples are mainly characterized by the presence of carbonate and hydrogen sulfate ions and by Kaolinite (absorption at 914 and 1010 cm^{-1}), while in samples with air masses coming from the NE, OC is mainly characterized by aliphatic and aromatic C-H and O-H and N-H groups (absorptions in the range 3500-2700 cm^{-1}) and by the presence of organonitrate, aromatic amide and amine and carboxylic acids (absorptions at 1630 and 1770-1700 cm^{-1}).

keywords: PM2.5, PM10, Organic Carbon and Elemental Carbon, Secondary organic aerosol, ATR-FTIR, dust.

1. Introduction

In urban and rural locations, carbonaceous compounds are an important fraction of atmospheric particulate matter (PM) (Hildemann et al. 1994; Putaud et al. 2004; Zhang et al. 2004). In fact, it generally accounts between 10 – 43% of PM10 and 21-78% of PM2.5. Carbonaceous PM is composed of elemental carbon (EC), which is a refractory component, and organic carbon (OC). The latter is generally present in large amounts in atmospheric aerosols. The organic fraction is composed of saturated and unsaturated aliphatic compounds, alcohols, aldehydes, ketones, carboxylic acids, aromatic compounds, amines, sugars, polyols and organic sulfur compounds (Seinfeld and Pandis 2016). Organic molecules can contribute to the Primary Organic Aerosol (POA) and Secondary Organic Aerosol (SOA). POA is directly emitted into the atmosphere and can originate from geological and natural sources, combustion and industrial emissions. SOA is formed either by homogenous oxidation and subsequent condensation of organic species in the gas phase or by heterogeneous oxidation in the aerosol phase (Robinson et al. 2007; Khan et al. 2016). Secondary Organic Aerosol is typically characterized by a higher oxidation degree, containing molecules with oxygenated functional groups, such as hydroxyl and carbonyl groups (Kawamura and Ikushima 1993; Kawamura and Yasui 2005). It is reported in literature that aged aerosols are expected to show a high content of oxygenated functional groups with the presence of SOA in a higher concentration than POA. These aerosols are then characterized by high organic matter to organic carbon mass ratio (Aiken et al. 2008; Turpin and Lim 2001).

Instead, EC is a primary pollutant, because it is mainly released in atmosphere from incomplete combustion of carbon-containing fuels.

Due to the relevant importance of the carbonaceous fraction of PM, many recent studies have been carried out, but its chemical characterization and formation mechanisms are not fully understood and have not studied in depth (Khan et al. 2016). Moreover, the quantification of SOA and POA is a point of strong debate; several indirect methods have been reported for their estimation and the EC-tracer method is a widely used technique (Turpin and Huntzicker 1995; Castro et al. 1991; Lim and Turpin 2002; Harrison and Yin 2008; Genga et al. 2017).

As described by Castro et al. (1991), this technique may give correct estimates of SOA if: the amount of SOA is negligible in samples used to calculate OC/ECmin ratio; the composition of primary fossil fuel carbonaceous sources is temporally and spatially constant; the contribution of other primary OC and EC sources is small. Frequently this is not the case, such as in receptor sites where biomass burning and bio aerosol primary

sources could be present. It has to be pointed out that due to diverse primary emissions the definition of a unique (OC/EC)prim ratio can lead to large uncertainties. Moreover, biomass burning leads to a high OC/EC ratio; therefore estimation of secondary OC from such a ratio could lead to over estimation regarding its contribution to particulate mass and total carbonaceous species (Querol et al. 2013; Pio et al. 2011; Genga et al. 2017). Notwithstanding, the EC-tracer method can serve as a suitable first order approach to estimate secondary OC.

In literature, several papers can be found on the study of carbonaceous fractions of particulate matter in the Italian peninsula (e.g., Lonati et al. 2007; Perrone et al. 2011; Sandrini et al. 2014; Khan et al. 2016; Genga et al. 2017) and also across Europe (Pio et al. 2011; Putaud et al. 2004; Putaud et al. 2010), but data available for Southern Italy are quite limited. The Apulia region is in the South of Italy and it is located in the center of the Mediterranean Sea. Due to the particular position of this site, the study of particulate matter is very interesting. In fact, in the Mediterranean Basin the sources and the composition of PM are very complex due to the presence of human activities in the industrialized regions, the transport of desert dust from northern Africa and the anthropogenic activity on the sea itself.

The purposes of this study are: to quantify the trend of carbonaceous aerosols during the day and in the warm season; to study the correlation existing among some meteorological parameters on carbonaceous PM concentration; to evaluate the secondary organic carbon in PM; to obtain information on the composition of the carbonaceous PM studying OC and EC levels, the functional groups of carbonaceous matter, and to account for the potential effect of long-range transports on them.

In order to study the functional groups present in carbonaceous aerosols, ATR-FTIR analysis has been performed. FTIR coupled with attenuated total reflectance (ATR) is a new technique developed recently and it allows for the direct analysis of samples without further preparation. Moreover, it has the ability to detect compounds in small quantities (Takahama et al. 2016). It should be pointed out that, while isolated molecules show absorption bands characterized by a series of narrow peaks, spectra of condensed phase show peaks significantly overlapping due to heterogeneous broadening of bands from similar bonds vibrating in slightly altered chemical environments (Kelley 2012). This is the case for atmospheric PM, as it comprises a mixture of many different components, with the organic fraction alone consisting of thousands of different types of molecules (e.g., Hamilton et al. 2004). This evidence poses challenges for interpretation and quantification.

For this purpose, a monitoring campaign was carried out; in particular 24-h and 6-h sampling campaigns have been performed. Elemental carbon and organic carbon concentration levels in PM10 and PM2.5 collected samples are presented and discussed.

2. Material and methods

2.1 Sampling site and devices

The sampling site was located in the Brindisi rural coastal area, in the Apulia region (south-eastern part of Italy). The area around the sampling site (BR rural) was highly agricultural and the sampling site was about 12 km south of the city of Brindisi. It was located 0.7 Km away from the sea at an elevation of 30 m a.s.l. The four lane motorway “Strada Statale 613” is located around 1 km away. A one month campaign (September 17th – October 16th) was carried out with the aim of characterizing PM10 and PM2.5 on a daily basis, and PM2.5 on a 6-hour basis.

FAI Instruments Hydra Dual Channel samplers were used for particulate matter collection on 47-mm-diameter pre-heated quartz substrates. PM mass concentrations were determined by the gravimetric method, conditioning substrates before and after sampling (at 25 °C for 48h and 50% humidity). The uncertainties on mass concentrations are lower than 5%.

2.2 OC and EC analysis

In this study, elemental and organic carbon were measured by Sunset Laboratory Thermal–Optical Carbon Aerosol analyzer (Birch and Cary 1996) with NIOSH protocol (NIOSH 1998; Genga et al. 2017). A 1.5 cm^2 punch of the quartz substrates was analyzed. For the determination of OC and EC, the NIOSH protocol proceeds in two phases. First, in an atmosphere of pure helium, carbon is volatilized by four temperature steps for OC determination. Afterwards, in a mixture of oxygen and helium, the carbon, which remains on the filter, is heated and oxidized in six temperature steps allowing EC determination. The carbonaceous substances evolved from the filter are quantitatively oxidized to carbon dioxide and subsequently reduced to methane, then they are detected with a high

sensitively flame ionization detector (FID). Uncertainties in EC and OC measurements are of the order of 5%. A denuder was not used during sampling, leading to a net positive bias of 3.7% (Genga et al. 2017).

2.3 ATR-FTIR analysis

Attenuated total reflectance-Fourier transform infrared (ATR-FTIR) spectroscopy ATR-FTIR spectra were obtained using a Vertex 70 FTIR spectrometer from Bruker. The measurements were carried out in ATR mode using a multiple reflection ATR accessory (Benchmark from SPECAC, UK) with horizontal geometry, equipped with a ZnSe crystal. ATR-FTIR spectra were obtained in the spectral region 400-4000 cm^{-1}. The resolution was 2 cm^{-1} and the number scans was 100 for each spectrum. All spectra presented were baseline corrected. Filters were scanned before and after sampling.

2.4 Statistical analysis

Multivariate statistical analysis was performed on data obtained from 6 hour PM2.5 samples. Principal Component Analysis (PCA) was used with the purpose of finding PM samples with similarity in chemical composition, using mathematical functions which best describe the relative distances between the samples. In this work Statistica 10.0 tools were used to perform PCA. Before applying PCA the following conditions were tested: 1. normal distribution of data; 2. redundancy of the variables used to discriminate between groups; 3. homogeneity in the variance/covariance matrices of variables across groups .

3. Results and discussion

3.1 Overview on results

In Table 1 means and deviation standards of concentrations of PM10 and PM2.5 sampled for 24 hours, Total Carbon (TC) and Total Carbonaceous Aerosols (TCA) at the rural site during the warm period from 17th September to 16th October 2015 are reported. PM10 concentrations varied from 6.8 to 62.6 μg m^{-3} with a mean value of 22 ± 14 μg m^{-3}, while PM2.5 concentrations varied from 2.8 to 28.0 μg m^{-3} with a mean value of 11 ± 6 μg

m^{-3}. Other sites of the Apulia region show PM levels comparable to the concentrations observed, as reported in Contini et al. (2014). The highest PM10 values were reached on 17th, 18th and 19th of September, in which the mass concentration threshold, fixed by European Union and Italian Law at 50 μg m^{-3}, was exceeded (EU-Directive 2008/50/CE). On 18th of September the PM2.5 threshold was exceeded, too.

Figure 1 shows PM10 mass concentrations versus the corresponding PM2.5 mass concentrations: the regression line equation is reported as well. It can be noted that PM2.5 and PM10 increase linearly and are well correlated ($r=0.91$, $p<0.05$). The dependence of PM10 on PM2.5 is generally an index of common emission sources which influence both PM fractions; this evidence was also seen in another sub urban site in the near province of Lecce (Perrone et al. 2016).

The amount of total carbon, both organic and elemental carbon inside each sample was evaluated (Table 1). It can be noted that the carbon content (Total Carbon TC) represents a considerable fraction for both PM10 and PM2.5. During sampling days, TC shows average values of 24 wt% and of 34 wt% for PM10 and PM2.5, respectively. In particular, in PM10 OC varied from 1.06 to 18.32 μg m^{-3} (mean concentration: 5 ± 4 μg m^{-3}, corresponding to 22 wt% of the total PM10); EC varied from 0.11 to 0.88 μg m⁻3 (mean value: 0.41 ± 0.19 μg m^{-3}, corresponding to 2 wt% of the total PM10). In PM2.5, OC varied from 0.54 to 12.91 μg m^{-3} (mean concentration: 3.5 ± 2.8 μg m^{-3} accounting for 31 wt% of the total PM2.5) and, finally, EC varied from 0.11 to 0.85 μg m^{-3} (mean value: 0.35 ± 0.18 μg m^{-3} contributing to 3 wt% of the total PM2.5).

The concentration levels and the trend observed are in agreement with the results obtained in other rural sites in the Italian peninsula (Sandrini et al. 2014) and European areas (Pio et al. 2011; Querol et al. 2008; Querol et al. 2004; Samara et al. 2014).

They show that, for urban-background sites of southern Europe, the (OC+EC)/PM10 ratio varies from 10% up to about 20% for PM10 mass concentrations varying within the 10–70 μg m^{-3} range. While, the (OC+EC)/PM2.5 ratio varies from 20% up to about 40% for PM2.5 mass concentrations, which is in accordance with the results of this study.

As expected, the EC values measured in the studied rural Brindisi (BR rural) site are lower than that reported for urban sites, only due to the primary nature of EC emissions.

As shown in Figure 2, OC gives the greatest contribution to the Total Carbon in both PM fractions. Moreover, it is clear that organic carbon is mostly distributed in the fine fraction (70 wt%), and EC is mainly fine (89 wt%).

This could be related to the origin of OC and EC. As is known in literature (Pio et al. 2011), EC is primary and it is mainly due to incomplete combustion, which releases sub-micrometric particles characterizing the fine fraction of PM (Smekens et al. 2005). For this reason, EC is considered a tracer for emissions from biomass burning sources and fossil fuel combustion sources (road transport). Instead, OC could be generated: 1) from incomplete combustion activities, which can be the source of sub micrometric particles (Thorpe and Harrison 2008), and 2) from biological particles (plant debris, pollen, etc.) mainly present in the coarse fraction (Bauer et al. 2002).

3.2.1 OC/EC ratio

The OC/EC ratio in PM10 varies from 4.3 to 25.1 (mean value: 11.3), while in PM2.5 it varies from 3.6 to 19.6 (mean value: 9.2). The higher values observed during summer, which are similar to those observed at other rural sites in Italy (Sandrini et al. 2014), may be due to a regional influence of SOA coming from anthropogenic and biogenic sources. Moreover, in both PM10 and PM2.5 a good correlation between OC and EC is also observed ($r=0.81$, $p<0.005$ for PM10 and $r=0.83$, $p<0.005$ for PM2.5).

The positive but scattered correlation shown (Fig. 3) could be due to a predominant POA source with variable OC/EC emission factors, or to a mix of POA and SOA which tend to correlate because of a similar transport pattern from the sources to the receptor site. In the POA/SOA model based on the OC/EC ratio, the presence of a predominant primary organic source (e.g., emissions from vehicles, biomass combustion, etc.) is suggested (Na et al. 2004). While, secondary organic carbon in addition to primary organic carbon has to be considered where the OC/EC ratios show higher values.

It is worth noting that OC/EC mean ratio is higher for PM10 than for PM2.5, indicating and confirming that EC is mainly fine, while there is an OC portion that is present in the coarse PM.

3.2.2 Secondary organic aerosol estimation

The estimation of primary and secondary organic carbon (OC_{prim} and OC_{sec}, respectively) is largely dependent on the applied methodology and a direct measurement is not possible. In this paper, the OC/EC minimum ratio method was used to evaluate the secondary organic carbon concentrations from the measured EC (Turpin and Huntzicker 1994; Pio et al. 2011; Querol et al. 2013; Genga et al. 2017), using equation (1):

$$OC_{meas}=[(OC/EC)_{min}*EC_{meas}]+OC_{sec} \quad (1)$$

where OC_{meas} and EC_{meas} are the measured organic and elemental carbon, and $(OC/EC)_{min}$ is defined as the minimum ratio observed in aerosol samples collected from the sampling site.

The $(OC/EC)_{min}$ ratio was estimated through the graphical method, called “EC tracer” method, as shown in Figures 3 a and b (Pio et al. 2011). To confirm the results obtained, a sensitivity test was performed with all the data, first by sorting the OC/EC ratio values of the data and then by choosing the lower 5% ratio value samples, with a minimum of three samples for small datasets. The obtained values are in agreement with those derived by the “EC tracer” method, so the latter was used. The minimum ratio was 4.8 for PM10 and 4.7 for PM2.5. The good agreement between the two calculated $(OC/EC)_{min}$ ratios suggests the same carbonaceous source for PM10 and PM2.5 in this site. It has to be said that carbonate may also be present as additional aerosol carbon, even if it is usually a small amount (Seinfeld and Pandis 2016), this may cause an over estimation of OC and then OC_{sec}.

As is shown in Figure 4 a and b, where $(OC/EC)_{min}$ ratios versus EC_{mean} is reported for different European sites differentiated in urban (background, kerbside and tunnel), industrial, rural and remote, the studied site (BR rural) presents values in the range of those reported for rural sites. This evidence may be due to a joint contribution of local emissions and regional transport, where the importance of regional and long range transported OC_{sec} is greater and $(OC/EC)_{min}$ ratios are higher. In fact, in Figure 4 it can be seen that the $(OC/EC)_{min}$ ratios have lower values where there are higher average EC concentrations, contrary to sites with lower pollution levels. This tendency seems to reflect the regional transport of primary and secondary OC to rural and remote areas, along with the higher relevance of EC emissions from fossil fuel combustion in urban areas.

The mean primary and secondary organic carbon concentrations in PM10 fractions are 3.04 μg m^{-3} and 1.97 μg m^{-3}, respectively; while in PM2.5 they are 1.95 μg m^{-3} and 1.59

μg m^{-3}, respectively. Primary organic carbon is composed by 81 wt% of fine fraction, while secondary organic carbon is composed by 65 wt% of fine fraction.

3.2.3 Variation of carbonaceous aerosol on a 6 hour basis

Figure 5a shows the variation of OC and EC mass concentration in PM2.5 samples each collected for 6 hours. It clearly appears that OC concentration increases at night and decreases during the day. This may be due to synergic effect of the lower temperature at night and increase of the boundary layer during the warmer part of the day. The first effect promotes the transfer of semi-volatile organic compounds to the solid phase, leading to adsorption on particles (khan et al. 2016). This causes the increase of the organic component concentration during night and then the decrease of the concentration of OC during the central hours of the day. The increase of the boundary layer is confirmed by the change in the wind speed shown in Figure 5b: from 08:00 to 18:00 local time the wind speed increases corresponding to a dilution of organic carbon. We should consider that in rural areas the difference between night and day is less evident than in urban areas, where emission sources, like vehicular traffic, are closer.

Despite the high variability of EC data, EC seems to increase in the early hours of the morning (06:00-12:00), probably due to local emissions, after which the concentration trend is similar to OC, decreasing with the increasing of the wind speed and increasing again during the evening when the wind speed is minimum.

In this paper we have differentiated carbonaceous compounds in organic carbon and elemental carbon and measured them by a thermo-optic analyzer. The thermograms are characterized by the presence of 11 peaks, namely OC1, OC2, OC3, OC4, Pyrol, EC1, EC2, EC3, EC4, EC5 and EC6. Considering the single peaks of the thermogram used to measure OC and EC, it clearly appears that the peaks from OC1 to EC2 show the same trend observed for OC (Fig. 6), while the EC3, EC4, EC5 and EC6 peaks present the behavior of EC.

The normality of the data was tested before performing statistical analysis on data of the 6 hour samples. Histograms and boxplots were drawn and Shapiro-Wilk test was applied (assumption $p<0.05$ not met). The results show that data of OC, EC, OC_{sec} and OC_{prim} were not normally distributed. Consequently, LogOC, LogEC, $LogOC_{sec}$ and $LogOC_{prim}$

were used instead OC, EC, OC_{sec} and OC_{prim} for statistical analysis. A positive statistical correlation between OC and EC was confirmed for all data (Table 2 a, b and c), as also shown in paragraph 3.2.1 for the 24 hour samples. OC, EC, OC_{prim} and OC_{sec} showed a negative relationship with wind velocity. This is probably due to the clearing and diluting function of wind (Pindado et al. 2009) and also to the variation of the boundary layer (Ferrero et al. 2010; Pecorari et al. 2013), as discussed in the previous paragraph.

The correlation with temperature was positive but not so high. A positive correlation between OC and temperature may be due to the contribution of the secondary organic carbon (Grivas et al. 2004).

It is well known that carbonaceous particulate matter (PM) is more complex than its inorganic counterparts because it contains a large number of compounds, is emitted from biogenic and anthropogenic sources, and can be created or transformed in the atmosphere (Seinfeld and Pandis 2016). Even if the knowledge of the molecular composition has increased, it is not clear which mixture of compounds constituted each peak of the thermogram, but surely they could be differentiated by volatility and oxidizability, in decreasing order from OC1 to EC6. Moreover, recent studies have been aimed at investigating the associations between OC-EC sub-fractions and health outcome (Wagner Et al. 2014), because many studies indicate that short-term exposure to carbon-containing particles is associated with more adverse health effects compared to exposure to undefined particulate matter (PM2.5 and PM10) (Janseen et al. 2011; Mauderly et al. 2011).

In order to study the possible variation in chemical composition of the particulate matter during the day, Principal Component Analysis (PCA) was carried out using sub-fraction of OC and EC derived by each thermogram (namely OC1, OC2, OC3, OC4, Pyrol, EC1, EC2, EC3, EC4, EC5 and EC6). PCA allows us to investigate similarities and differences among 6 hour PM2.5 samples. Normality of the data was tested observing histograms, boxplots and applying the Shapiro-Wilk test (assumption $p<0.05$ not met) before applying statistical analysis: OC1, OC2, OC3, EC1, EC2 and EC3 did not show normal distribution. Redundant variables were eliminated and a logarithmic transformation was applied to OC1, OC2, OC3, EC1, EC2 and EC3. Chemical parameters (OC1, OC2, OC3, OC4, Pyrol, EC1, EC2, EC3, EC4) provided data sets structured in a multidimensional matrix (9 variables for 130 samples), which were subjected to multivariate statistical treatment using the software package STATISTICA 10.0.

The score plot in the sub-space of the first three Principal Components (PCs), explaining 93% of total variance, is shown in Figure 7. The ellipses corresponding to a 95% confidence limit are also drawn in Figure 7 and their areas can be assumed to define clusters boundaries. In table 3 factor loadings of the original variables are reported. It is well evident the high correlation among OC1, OC2, OC3, Pyrol, EC2, EC3 fractions, confirming the correlation between the total OC and total EC pointed out in paragraph 3.2.3. Instead, the OC4 fraction shows coordinates different from the other ones.

Examining Figure 7, analyzed samples are clustered into two well defined clusters (1 and 2). Analyzing each sample belonging to the two different clusters, it can be seen that cluster 2 includes samples collected on 17th, 18th and 19th of September, while cluster 1 includes all the other samples. It can be noted that these two clusters are mainly separated along the PC2 and the loading analysis (Table 3) explains that the discrimination along PC2, leading to separation of cluster 1 from cluster 2, is due to the contribution of OC4. It can be said that OC4 differentiates samples of cluster 2 from samples of cluster 1. Perrone et al. (2011) observed in samples collected in Lecce, a site not so far from the studied site, that the peak of the thermogram which occurs within the 220-250 s time interval could be due to the presence of carbonates besides organic carbon. As the fourth temperature step (OC4) occurs in the range 220-250 s time, it is probably due to the presence of carbonate ions besides other organic components. And so it is possible that the presence of carbonates leads to a differentiation between the two clusters.

Moreover, it can be noted that in cluster 1 along PC3 the PM sampled in the 06:00-12:00 range time are differentiated from the PM sampled in 12:00-18:00 range, this is due to the higher positive loading of EC1 and higher negative loading of EC4. Instead, samples from the 00:00-06:00 and 18:00-24:00 range are spread over the entire cluster 1, showing no particular differentiation.

This evidence may suggest that the PM collected in the two different time ranges (06:00-12:00 and 12:00-18:00 hours) are well characterized by different chemical composition and that the main difference is due to two fractions, mainly EC1 and EC4.

3.3 Discussion of specific pollution events

In Figure 8a the trend of PM10 and PM2.5 concentrations is shown. A considerable increase in concentration during the days 17th, 18th, 19th September was observed, when the threshold of 50 μg m^{-3} prescribed by the Italian law for PM10 was exceeded. The same trend has been observed in other cities of the Apulia region (Fig. 8b) monitored by the environmental protection agency (ARPA Puglia). This evidence suggests that, during the days with high concentration values, an atmospheric phenomenon affecting the whole region occurred and was, therefore, not due to local sources. Moreover, these days in September are characterized by an increase of the coarse fraction (PM2.5/PM10 ratios showing values between 0.43 and 0.46 (Fig. 8a)). This evidence could be due to a Saharan dust event. In fact, the Italian peninsula is characterized by presence of natural particles mainly belonging to Sahara-Sahel desert (Perrone et al. 2016; Rodriguez et al. 2002; Mallone et al. 2011; Peteraki et al. 2002), and it was reported by Perrone et al. (2016) that this event has the greatest impact on PM10 because Saharan dust is essentially characterized by coarse particles.

To confirm this hypothesis, 7-days back-trajectories were evaluated with Hysplit. Figure 9 (only the back-trajectories of 17th September are reported as an example, *http://aeronet.gsfc.nasa.gov/*) shows that this event is associated with a transport from the SW direction, belonging to the North Africa region. Moreover, in Figures 10 a and b, the map of the dust load, obtained from the BSC-DREAM8b model, and the vertical profile, obtained by Dust Regional Atmospheric Model (DREAM) developed by Euro-Mediterranean Centre on Insular Dynamics (ICoD), are reported. These figures highlight the presence of a dust load on the entire Italian peninsula (as an example the map for the sampling day 17th September is shown in Figure 10a and the presence at ground level in Lecce. Back trajectories indicate extensive transport of air masses from the southeast on 17th, 18th, 19th September, thus confirming Saharan Dust events, while during the remaining sampling days Saharan Dust events were not observed.

Moreover, the OC and EC mean mass concentrations are slightly greater in dust-affected samples than in dust-free samples (Fig. 11); in fact, it can be noted that during the days 17th, 18th, 19th September there was an increase of OC and EC. It can be also seen that the mean OC/EC ratio, that is equal to 16 ± 5 and 14 ± 2 in dust-affected PM10 and PM2.5 samples, respectively, decreases to 10 ± 3 and 8 ± 3 in dust-free PM10 and PM2.5 samples, respectively. This last evidence could be explained by the smaller impact of traffic sources and fossil fuels on the long-range air masses that transport African dust

(Perrone et al. 2016) and by the increase of OC compound in these events. Furthermore, in the previous paragraph it was pointed out that the OC4 fraction leads to a differentiation of dust from dust free samples. The hypothesis that OC4 can be partially composed by carbonates is supported by the fact that these latter compounds are considered good tracers for Saharan dust. This is because carbonates, such as calcite and dolomite, are found in the North African deserts of Libya, Algeria and Tunisia increasing the levels of carbonates during Saharan dust episodes (Formenti et al. 2008).

Furthermore, OC_{sec} and OC_{prim} values are larger in dust-affected samples than in dust-free samples. It has to be said that the increase of OC on a dusty day could be due to the presence of carbonate, as supposed in the Principal Component Analysis results. OC_{sec} is equal to 6.9 ± 1.2 and 5.1 ± 0.3 in dust-affected PM10 and PM2.5 samples, respectively, and it decreases to 2.2 ± 2.2 and 1.5 ± 1.3 in dust-free PM10 and PM2.5 samples, respectively. OC_{prim} is equal to 3.1 ± 0.5 and 2.4 ± 0.3 in dust-affected PM10 and PM2.5 samples, respectively, and it decreases to 1.8 ± 0.6 and 1.6 ± 0.5 in dust-free PM10 and PM2.5 samples, respectively. This is in accordance with the trend for OC/EC ratio in dust-free samples and in dust-affected samples, as already described.

The maximum concentration of OC and EC (Fig. 11), and also of OC_{sec} and OC_{prim} values was measured 2nd October. On this day, instead, back trajectories indicate that air masses belong to Northeastern Europe (Fig. 12). In literature it is stated that, with air masses belonging to Northeastern Europe, secondary aerosol concentration increases (di Gilio et al. 2015). In fact, in literature it is stated that, Long Range Transport (LRT) appears to play a dominant role in the air pollution in southern Italy, which is characterized by a higher planetary boundary layer than that observed in Northern Italy, especially in summer. This is a common characteristic of countries bordering the Mediterranean basin (di Gilio et al. 2015 and therein references). Moreover, di Gilio et al. have evaluated the LRT in the Apulia region, by the means of three-dimensional four-day BTs computed every hour and then performing cluster analysis, and they have observed that when the air masses belong to Northeastern Europe the secondary aerosol concentration increases (di Gilio et al. 2015).

20th September and 10th October, when an enrichment of coarse particles was measured (Fig. 8a), the back trajectories show that the increase of PM concentrations in the atmosphere is due to air masses belonging to the ocean and thus, probably, to the presence of sea spray coarse particles.

3.4 ATR-FTIR analysis

Fourier transform infrared coupled with attenuated total reflectance (ATR-FTIR) spectroscopic method was used to determine functional groups. The representative ATR-FTIR spectra of the PM samples collected on Quartz filters during Saharan dust days (19th September), the day with the lowest value of OC_{sec} (28th September) and that with the highest value of OC_{sec} (2nd October with winds blowing from NE) are shown in Figure 13.

In table 4 the identified organic functional groups and inorganic ions are reported. (Cucciniello et al. 2013).

The peaks around 1065 and 800 cm^{-1} in IR spectra of both PM10 and PM2.5 samples are mainly due to the quartz filter. In particular, the band at 1065 cm^{-1} was due to asymmetrical stretching vibration of O-Si-O (Maria et al. 2002) and the peak at 800 cm^{-1} was assigned to the bending vibration of O-Si-O both present in the silicate ions (SiO_4^{4-}) (Gilardoni et al. 2009). Within the spectra of PM10 and PM2.5 collected during the Saharan dust event, a weak shoulder at 1010 cm^{-1} appeared (Fig. 13b) and it was attributed to absorbance of kaolinite ($Al_2Si_2O_5(OH)_4$). In the same samples, an additional peak appeared at 914 cm^{-1}, Ravisankar et al. (2010) show that this peak was due to vibrations of Al-(OH) which are present in the octahedral structure of kaolinite. These signals are more pronounced in the PM10 sample than the PM2.5 because it is richer in coarse dust. The presence of the kaolinite absorbance confirms the Saharan dust event; in fact Shaka' and Saliba (2004) observed the presence of the kaolinite in IR spectra of samples collected in a sandy day on Beirut (Lebanon). The appearance of a shoulder band between 1410 and 1435 cm^{-1} and the peak at 870 cm^{-1} (Fig. 13 b and c) were due to asymmetric vibrations of $CaCO_3$, these signals are more marked in the ATR-FTIR spectra of coarse dust PM than in spectra of dust free samples. This evidence might indicate and confirm the presence of dust particles transported and generated by the wind (Shaka ’ and Saliba 2004, Perrone et al. 2011; Anıl et al. 2014). The presence of sulfate ions can be recognized in all the samples, with bands at 1134 and 600 cm^{-1}. Moreover, the asymmetrical stretching vibration of the sulfate ions is responsible for the shoulder about 1087 cm^{-1}. Furthermore, in Figure 13b the shoulders at 560, 830, 1087 and 1179 cm^{-1}, attributed to hydrogen sulfate ions are easily recognizable even if they are more evident in the dust PM10 spectrum.

Aliphatic and aromatic C-H and O-H and N-H bonds are responsible for the absorption in the range 3500-2700 cm^{-1} (Fig. 13d). These signals are mainly present in the sample with NE winds, where, as previously reported, the highest values of OC and OC_{sec} were observed. O-H stretching vibration of water or alcohol leads to the broad shoulder at 3400 cm^{-1} (Coury and Dillner 2008). The presence of C-OH group in PM samples may be due to alcohols, polyols, and sugars that are originated from biogenic emissions and biomass burning. In fact, the anhydro-sugar levoglucosan is used as a tracer of biomass burning, and it could reach more than 10 wt% of the organic carbon originating from wood combustion (Anil et al. 2014 and therein references). The burning of charcoal may lead to a higher presence of aromatic compounds, too (Cucciniello et al. 2015). The water present in PM can be recognized by peaks at 3400 and 1620 cm^{-1}.

Moreover, still looking at the spectrum of the NE sample, the presence of ammonium is responsible for the broad signal in the region 2800-3200 cm^{-1}. This band overlaps some of the organic functional group signals. The stretching vibrations of N-H bonds of ammonium lead to bands at 3230 and 3040 cm^{-1}. The asymmetric and symmetric stretching of aliphatic CH_2 groups is responsible for the absorptions at 2920 and 2850 cm^{-1}, while the stretching of aliphatic CH_3 groups is responsible for the peak at 2960 cm^{-1}. The aliphatic carbon (saturated aliphatic C-C-H) may contribute to the band at 1450 cm^{-1}

The shoulder at 1630 cm^{-1} corresponds with absorption of organonitrate, aromatic amide and amine organic functional groups. Instead, the vibrations of the carbonyl group (C=O) of the carboxylic acids are responsible for the shoulder between 1770 and 1700 cm^{-1}. Anil et al. (2014) suggested that these compounds were produced by photo-oxidation of anthropogenic and biogenic compounds. It can be seen in Figure 13c, that these signals are more intense in samples collected when the winds blow from the NE than from the other directions.

Finally, nitrate ions absorbs at 1350 cm^{-1}, confirmed by the shoulder at 820 cm^{-1}, while the shoulder at 1420 cm^{-1} was attributed to the NH_4^+ (Allen et al. 1194; Maria et al. 2003). Once again, these signals are more evident in the spectrum of NE sample (2nd October sample).

Conclusions

The sampling campaign, carried out from 17th September 2015 to 20th October 2015, has shown that the carbon content represents a large part of both PM10 and PM2.5, in

accordance with other rural sites of southern Europe. OC and EC found in PM10 in amounts of 22 wt% and 2 wt%, respectively, shows that OC is the greatest part of the Total Carbon. Instead OC and EC are found in PM2.5 in amounts of 31 wt% and 3 wt%, respectively. Moreover, it is clear that organic carbon is mostly distributed in the fine fraction and EC is mainly fine. This evidence is related to the sources of the carbonaceus species. In fact, EC is associated with incomplete combustion characterized by sub-micrometric particles (traffic emissions, biomass bourning), and OC to incomplete combustion and biological particles. The good correlation between OC and EC suggests the presence of a predominant primary organic source and where the OC/EC ratios show higher values, secondary organic carbon in addition to primary OC must also be considered. Moreover, the stable atmosphere, the lower temperature and lower mixing during night all play important roles for the accumulation of OC in PM fractions and promote condensation and adsorption of volatile organic compounds.

The studied site is also affected by long-range transport of aerosols, such as Saharan Dust phenomena, because countries bordering the Mediterranean basin are often downwind from African mineral dust plumes. During these events the OC_{sec} and OC_{prim} values are slightly greater than in dust free days. It should be pointed out that, as shown in PCA and in ATR-FTIR analyses, during these phenomena the PM samples are characterized by the presence of carbonate, which could be responsible for an overestimation of the organic carbon mainly in these days. The highest values of OC and EC, OC_{sec} and OC_{prim} were measured when the air masses come from Northeastern Europe. The presence of more oxidized organic compounds in OC_{sec}, when the winds blow from NE Europe, is shown by ATR-FTIR analysis. In the NE samples there was an increase of organic functional groups including non-acid organic hydroxyl C-OH group (sugars, anhydrosugars, and polyols, herein indicated as alcohol group), aromatic C=C-H group, aliphatic unsaturated C=C-H group, aliphatic saturated C-C-H group, non-acid carbonyl C=O group, carboxylic acid COOH group, and amine NH_2 group.

Acknowledgements

This research was supported by the Project PON 254/Ric. Potenziamento del “CENTRO RICERCHE PER LA SALUTE DELL'UOMO E DELL'AMBIENTE” Cod. PONa3_00334.

References

Aiken AC, De Carlo PF, Kroll JH, Worsnop DR, Huffman JA, Docherty KS, Ulbrich IM, Mohr C, Kimmel JR, Sueper D, Sun Y, Zhang Q, Trimborn A, Northway M, Ziemann PJ, Canagaratna MR, Onasch TB, Alfarra MR, Prevot ASH, Dommen J, Duplissy J, Metzger A, Baltensperger U, Jimenez JL (2008) O/C and OM/OC Ratios of Primary, Secondary, and Ambient Organic Aerosols with High-Resolution Time-of-Flight Aerosol Mass Spectrometry. Environ Sci Technol 42:4478–4485

Allen DT, Palen EJ, Haimov MI, Hering SV, Young JR (1994) Fourier transform infrared spectroscopy of aerosol collected in a low pressure impactor (LPI/FTIR): method development and field calibration. Aerosol Science and Technology 2 1 (4):25–342

Anıl I, Golcuk K, Karaca F (2014) ATR-FTIR Spectroscopic Study of Functional Groups in Aerosols: The Contribution of a Saharan Dust Transport to Urban Atmosphere in Istanbul, Turkey. Water Air Soil Pollut 225:1898

Bauer H, Kasper-Giebl A, Löflund M, Giebl H, Hitzenberger R, Zibuschka F, Puxbaum H (2002) The contribution of bacteria and fungal spores to the organic carbon content of cloud water, precipitation and aerosols. Atmos Res 64:109–119

Birch ME, Cary RA (1996) Elemental carbon-based method for monitoring occupational exposures to particulate diesel exhaust. Aerosol Sci Technol 25:221–241

Castro LM, Pio CA, Harrison RM, Smith DJT (1991) Carbonaceous aerosol in urban and rural European atmospheres: estimation of secondary organic carbon concentrations. Atmos Environ 33:2771–2781

Coury C, Dillner AM (2008) A method to quantify organic functional groups and inorganic compounds in ambient aerosols using attenuated total reflectance FTIR spectroscopy and multivariate chemometric techniques. Atmos Environ 42 (23):5923–5932

Cucciniello R, Proto A, Rossi F, Motta O (2013) Mayenite based supports for atmospheric NOx sampling. Atmos Environ 79:666-671

Cucciniello R, Proto A, Rossi F, Marchettini N, Motta O (2015) An improved method for BTEX extraction from charcoal. Anal Methods 7:4811

Di Gilio A, de Gennaro G, Dambruoso P, Ventrella G (2015) An integrated approach using high time-resolved tools to study the origin of aerosols. Sci Tot Environ 530–531:28–37

Ferrero L, Perrone MG, Petraccone S, Sangiorgi G, Ferrini BS, Lo Porto C, Lazzati Z, Cocchi D, Bruno F, Greco F, Riccio A, Bolzacchini E (2010) Vertically-resolved particle size distribution within and above the mixing layer over the Milan metropolitan area (Article). Atmos Chem Phys 10 (8): 3915-3932

Formenti P, Rajot JL, Desboeufs K, Caquineau S, Chevaillier S, Nava S, Gaudichet A, Journet E, Triquet S, Alfaro S, Chiari M, Haywood J, Coe H, Highwood E (2008) Regional variability of the composition of mineral dust from western Africa: Results from the AMMA SOP0/DABEX and DODO field campaigns. J Geophys Res 113:D00C13. doi:10.1029/2008JD009903

Genga A, Ielpo P, Siciliano T, Siciliano M (2017) Carbonaceous particles and aerosol mass closure in PM2.5 collected in a port city. Atmos Res 183:245–254

Gilardoni S, Liu S, Takahama SM, Russell L, Allan JD, Steinbrecher R, Jimenez JL, De Carlo PF, Dunlea EJ, Baumgardner D (2009) Characterization of organic ambient aerosol during MIRAGE 2006 on three platforms. Atmos Chem Phys 9:5417–5432

Grivas G, Chaloulakou A, Samara C, Spyrellis N (2004) Spatial and temporal variation of PM10 mass concentrations within the greater area of Athens, Greece. Water Air Soil Pollut 158:357–371

Hamilton J F, Webb PJ, Lewis AC, Hopkins JR, Smith S, Davy P (2004) Partially oxidised organic components in urban aerosol using GCXGC-TOF/MS. Atmos Chem Phys 4:1279–1290

Harrison RM, Yin J (2008) Sources and processes affecting carbonaceous aerosol in central England. Atmos Environ 42 (7): 413–1423

Hildemann LM, Mazurek MA, Cass GR, Simoneit BRT (1994) Seasonal Trends in Los Angeles Ambient Organic Aerosol Observed by High-Resolution Gas Chromatography. Aerosol Sci Tech 20:303–317

Janssen NA, Hoek G, Simic-Lawson M, Fischer P, van Bree L, ten Brink H, Keuken M, Atkinson RW, Anderson HR, Brunekreef B, Cassee FR (2011) Black carbon as an additional indicator of the adverse health effects of airborne particles compared with PM10 and PM2.5. Environ Health Perspect 119 (12):1691-9

Kawamura K, Ikushima K (1993) Seasonal changes in the distribution of dicarboxylic acids in the urban atmosphere. Environ Sci Technol 27:2227–2235

Kawamura K, Yasui O (2005) Diurnal changes in the distribution of dicarboxylic acids, ketocarboxylic acids and dicarbonyls in the urban Tokyo atmosphere. Atmos Environ 39:1945–1960

Kelley AM (2012) Condensed-Phase Molecular Spectroscopy and Photophysics. John Wiley & Sons.

Khan MdB, Masiol M, Formenton G, Di Gilio A, de Gennaro G, Agostinelli C, Pavoni B (2016) Carbonaceous PM2.5 and secondary organic aerosol across the Veneto region (NE Italy). Sci Tot Environ 542:172–181

Lim H, Turpin B (2002) Origins of primary and secondary organic aerosol in Atlanta: results of time-resolved measurements during the Atlanta supersite experiment. Environ Sci Technol 36:4489–4496

Lonati G, Ozgen S, Giugliano M (2007) Primary and secondary carbonaceous species in PM2.5 samples in Milan (Italy). Atmos Environ 41:4599–4610

Maria SF, Russell LM, Turpin BJ, Porcja RJ (2002) FTIR measurements of functional groups and organic mass in aerosol samples over the Caribbean. Atmos Environ 36(33):5185–5196

Mallone S, Strafoggia M, Faustini A, Gobbi GP, Marconi A, Forastiere F (2011) Saharan Dust and Associations between Particulate Matter and Daily Mortality in Rome, Italy. Environ Health Perspect 119:1409–1414

Mauderly Chow (2008) Health Effects of Organic Aerosols. Inhalation Toxicology 20:257–288

Na K, Aniket A, Sawant, Chen Song, Cocker III DR (2004) Primary and secondary carbonaceous species in the atmosphere of Western Riverside County, California. Atmos Environ 38:1345–1355

NIOSH: Method 5040 Cassinelli ME, O'Connor PF (Eds.), NIOSH: Manual of Analytical Methods (NMAM) (fourth ed.) (1998) [Suppl. 2, Supplement to DHHS (NIOSH) Publication No. 94-113]

Pateraki St, Assimakopoulos VD, Maggos Th, Fameli KM, Kotroni V, Vasilakos (2013) Particulate matter pollution over a Mediterranean urban area. Sci Tot Environ 463:508–24

Pecorari E, Squizzato S, Masiol M, Radice P, Pavoni B, Rampazzo G (2013) Using a photochemical model to assess the horizontal, vertical and time distribution of $PM_{2.5}$ in a

complex area: Relationships between the regional and local sources and the meteorological conditions. Sci Tot Environ 443:681–691

Perrone MR, Piazzalunga A, Prato M, Carofalo I (2011) Composition of fine and coarse particles in a coastal site of the central Mediterranean: Carbonaceous species contributions. Atmos Environ 45:7470-7477

Perrone MR, Genga A, Siciliano M, Siciliano T, Paladini F, Burlizzi P (2016) Saharan dust impact on the chemical composition of PM10 and PM1 samples over south-eastern Italy. Arab J Geosci 9:1-11

Pindado O, Perez R, Garcia S, Sanchez M, Galan P, Fernandez M (2009) Characterization and sources assignation of PM2.5 organic aerosol in a rural area of Spain. Atmos Environ 43:2796–2803

Pio C, Cerqueira M, Harrison RM, Nunes T, Mirante F, Alves C, Oliveira C, Sanches de la Campa A, Artinano B, Matos M (2011) OC/EC ratio observations in Europe: Re-thinking the approach for apportionment between primary and secondary organic carbon. Atmos Environ 45:6121-6132

Putaud JP, Raes F, Van Dingenen R, Brüggemann E, Facchini MC, Decesari S, Fuzzi S, Gehrig R, Hüglin C, Laj P, Lorbeer G, Maenhaut W, Mihalopoulos N, Müller K, Querol X, Rodriguez S, Schneider J, Spindler G, ten Brink H, Tørseth K, Wiedensohler A (2004) A European aerosol phenomenology—2: chemical characteristics of particulate matter at kerbside, urban, rural and background sites in Europe. Atmos Environ 38:2579-2595

Putaud JP, Van Dingenen R, Alastuey A, Bauer H, Birmili W, Cyrys J, Flentje H, Fuzzi S, Gehrig R, Hansson HC (2010) European aerosol pheneomenology–3: Physical and chemical characteristics of particulate matter from 60 rural, urban and kerbside sites across Europe. Atmos Environ 44:1308–1320

Querol X, Alastuey A, Ruiz CR, Artiñano B, Hansson HC, Harrison RM, Buringh E, Brink HM, Lutz M, Bruckmann P, Straehl P, Schneider J (2004) Speciation and origin of PM10 and PM2.5 in selected European cities. Atmos Environ 38:6547–6555

Querol X, Alastuey A, Moreno T, Viana MM, Castillo S, Pey J, Rodríguez S, Artiñano B, Salvador P, Sánchez M, Garcia Dos Santos S, Herce Garraleta MD, Fernandez-Patier R, Moreno-Grau S, Negral L, Minguillón MC, Monfort E, Sanz MJ, Palomo-Marín R, Pinilla-Gil E, Cuevas E, de la Rosa J, Sánchez de la Campa A (2008) Spatial and temporal

variations in airborne particulate matter (PM_{10} and $PM_{2.5}$) across Spain 1999–2005. Atmos Environ 42:3964–3979

Querol X, Alastuey A, Viana M, Moreno T, Reche C, Minguillon MC, Ripoll A, Pandolfi M, Amato F, Karanasiou A, Perez N, Pey J, Cusack M, Vazquez R, Plana F, Dall'Osto M, de la Rosa J, Sanchez de la Campa A, Fernandez-Camacho R, Rodrıguez S, Pio C, Alados-Arboledas L, Titos G, Artınano B, Salvador P, Garcıa Dos Santos S, Fernandez Patier R (2013) Variability of carbonaceous aerosols in remote, rural, urban and industrial environments in Spain: implications for air quality policy. Atmos Chem Phys 13:6185–6206

Ravisankar R, Kiruba S, Eswaran P, Senthilkumar G, Chandrasekaran A (2010) Mineralogical characterization studies of ancient potteries of Tamilnadu, India by FT-IR spectroscopic technique. E-Journal of Chemistry 7(s1):S185–S190. doi:10.1155/2010/643218.

Robinson A, Donahue NM, Shrivastava MK, Weitkamp EA, Sage AM, Grieshop AP, Lane TE, Pierce JR, Pandis (2007) Rethinking organic aerosols: semivolatile emissions and photochemical aging. Science 315:1259–1262

Rodriguez S, Querol X, Alastuey A, Mantilla E (2002) Origin of high summer PM10 and TSP concentrations at rural sites in Eastern Spain. Atmos Environ 36:3101–12

Samara C, Voutsa D, Kouras A, Eleftheriadis K, Maggos T, Saraga D, Petrakakis M (2014) Organic and elemental carbon associated to PM_{10} and $PM_{2.5}$ at urban sites of northern Greece. Environ Sci Pollut Res 21:1769–1785

Sandrini S, Fuzzi S, Piazzalunga A, Prati P, Bonasoni P, Cavalli F, Bove MC, Calvello M, Cappelletti D, Colombi C, Contini D, de Gennaro G, Di Gilio A, Fermo P, Ferrero L, Gianelle V, Giugliano M, Ielpo P, Lonati G, Marinoni A, Massabò D, Molteni U, Moroni B, Pavese G, Perrino C, Perrone MG, Perrone MR, Putaud JP, Sargolini T, Vecchi R, Gilardoni S (2014) Spatial and seasonal variability of carbonaceous aerosol across Italy. Atmos Environ 99:587-598

Seinfeld JH, Pandis SN (2016) Atmospheric chemistry and physics: from air pollution to climate change. Wiley, p 1326

Shaka' H, Saliba NA (2004) Concentration measurements and chemical composition of PM10–2.5 and PM2.5 at a coastal site in Beirut, Lebanon. Atmos Environ 38(4):523–531. doi:10.1016/j.atmosenv.2003.10.009.

Smekens A, Moreton Godoi RH, Berghmans P, Van Grieken R (2005) Characterisation of soot emitted by domestic heating, aircraft and cars using diesel or biodiesel(Article). J Atmos Chem 52 (1):45-62

Takahama S, Ruggeri S, Dillner AM (2016) Analysis of functional groups in atmospheric aerosols by infrared spectroscopy: sparse methods for statistical selection of relevant absorption bands. Atmos Meas Tech 9:3429-3454

Thorpe A, Harrison RM (2008) Sources and properties of non-exhaust particulate matter from road traffic: A review. Sci Tot Environ 400:270-282

Turpin BJ, Huntzicker JJ (1994) Investigation of organic aerosol sampling artifacts in the Los Angeles basin. Atmos Environ 28(19):3061-3071

Turpin BJ, Huntzicker JJ (1995) Identification of secondary organic aerosol episodes and quantification of primary and secondary organic aerosol concentrations during SCAQS. Atmos Environ 29:3527–3544

Turpin BJ, Lim HJ (2001) Species Contributions to PM2.5 Mass Concentrations: Revisiting Common Assumptions for Estimating Organic Mass. Aerosol Sci Tech 35:602–610

Wagner JG, Kamal AS, Morishita M, Dvonch JT, Harkema JR, Rohr AC (2014) PM2.5-induced cardiovascular dysregulation in rats is associated with elemental carbon and temperature-resolved carbon subfractions. Part Fibre Toxicol 11:25

Zhang X, Smith KA, Worsnop DR, Jimenez JL, Jayne JT, Kolb CE, Morris JW, Davidovits P (2004) Numerical characterization of particle beam collimation: Part II integrated aerodynamic-lens-nozzle system. Aerosol Sci Tech 36:619–638

http://aeronet.gsfc.nasa.gov/

www.arpa.puglia.it/web/guest/progtarantosalento

http://www.bsc.es/ess/bsc-dust-daily-forecast

Figure captions

graphical abstract

Fig. 1 PM2.5 versus PM10 mass concentrations

Fig. 2 Mass distribution (µg m^{-3}) of Organic Carbon (OC), Elemental Carbon (EC) and Total Carbon (TC) in PM10, PM 10-2.5 and PM2.5, bars indicate standard deviation

Fig. 3 OC versus EC for a) PM10 and b) PM2.5. The dashed line corresponds to the minimum ratio (OC/EC)min

Fig. 4 $(OC/EC)_{min}$ ratios found at urban, industrial, rural and remote locations in a) PM10 and b) PM2.5 aerosol samples (Pio et al. 2011; Jones and Harrison 2005; Viana et al. 2007; www.arpa.puglia.it/web/guest/progtarantosalento). Br rural is indicated with an arrow

Fig. 5 a) Mass distribution (µg m^{-3}) of organic carbon (OC) and elemental carbon (EC) in PM2.5 collected for 6 hours (00:00-06:00; 06:00-12:00; 12:00-18:00;18:00-0:00); b) mean variation of wind speed during the day in the sampling campaign

Fig. 6 Mass distribution (µg m^{-3}) of a) OC1, OC2, OC3, OC4 and Pyrol peak and b) EC1, EC2, EC3, EC4, EC5 and EC6 of thermogram in PM2.5 collected for 6 hours (00:00-06:00; 06:00-12:00; 12:00-18:00;18:00-0:00)

Fig. 7 Score plot in the sub-space of the first three principal components (PC1, PC2 and PC3) related to 6 hours PM 2.5 samples

Fig. 8 a) PM2.5/PM10 ratio and PM10 and PM2.5 concentration variations during sampling campaign; b) PM10 concentration in different city of Apulia region (South Italy) monitored by the environmental protection agency (ARPA) (www.arpa.puglia.it/web/guest/progtarantosalento)

Fig. 9 7-days Back Trajectories for the day 17th September **(**http://aeronet.gsfc.nasa.gov/)

Fig. 10 a) dust concentration distribution for the day 17th September from BSC-DREAM8b (Dust REgional Atmospheric Model)**,** by Barcelona Supercomputing Center (http://www.bsc.es/ess/bsc-dust-daily-forecast); b) vertical profile for the day 17th September from BSC-DREAM8b (Dust REgional Atmospheric Model)

Fig. 11 Trend of OC and EC concentrations (µg m^{-3}) for PM10 (OC10 and EC10, respectively) and PM2.5 (OC2.5 and EC2.5, respectively) during the sampling period

Fig. 12 7-days Back Trajectories for the day 2nd October **(**http://aeronet.gsfc.nasa.gov/)

Fig. 13 a) ATR-FTIR Spectra showing the bands of particles collected on quartz filters (black dust PM10, red dust PM2.5, blue dust free PM10, green dust free PM2.5, pink NE PM10 and grey NE PM2.5); b) magnification of the spectra region 500-1300 cm^{-1}, c) magnification of the spectra region 1300-2000 cm^{-1} and d) magnification of the spectra region 2400-4000 cm^{-1}. 2250-2400 cm^{-1} CO_2 interference region has been removed from the raw data

Figure

Click here to download Figure graphical abstract.tif

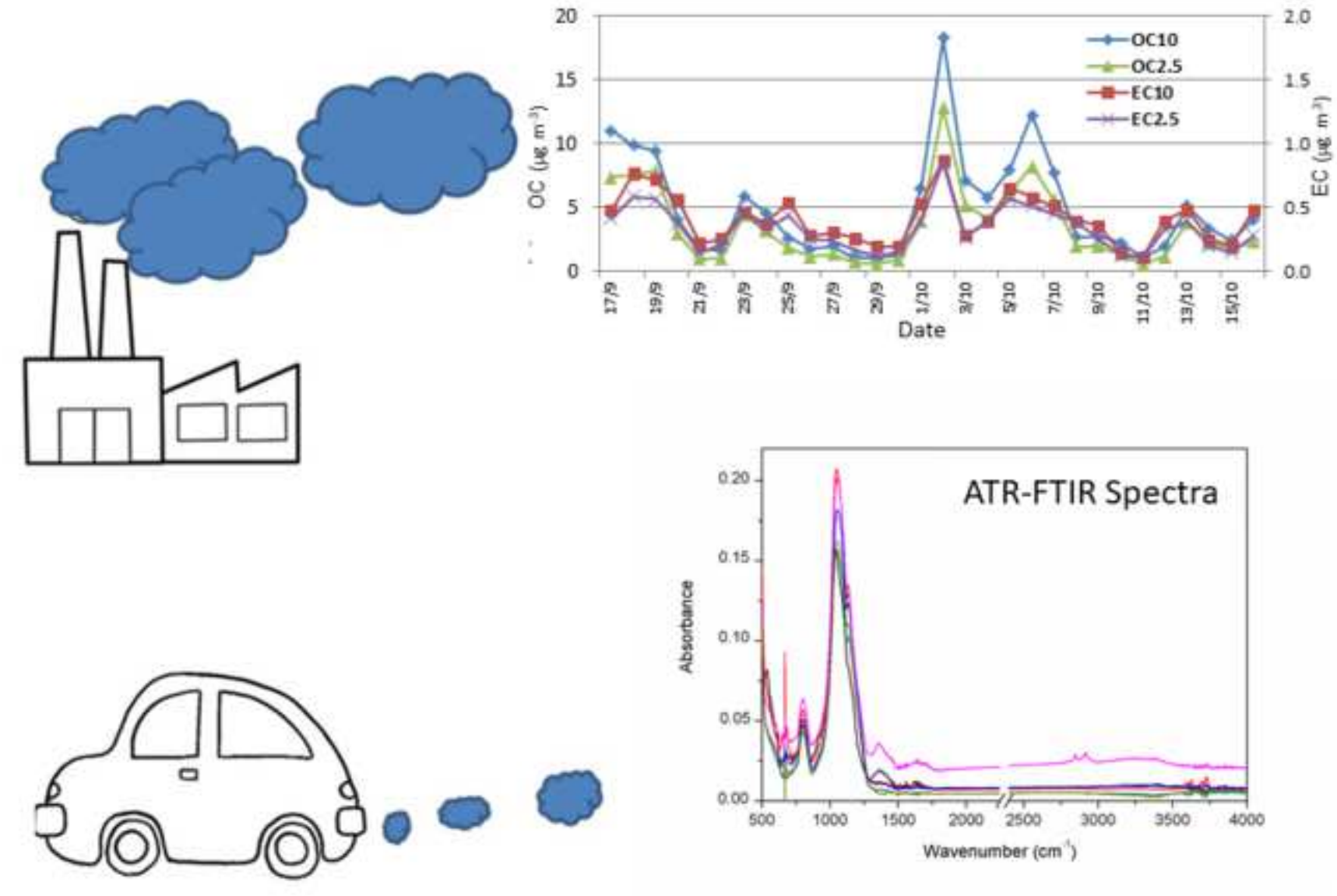

Figure

Click here to download Figure Fig 1.tiff

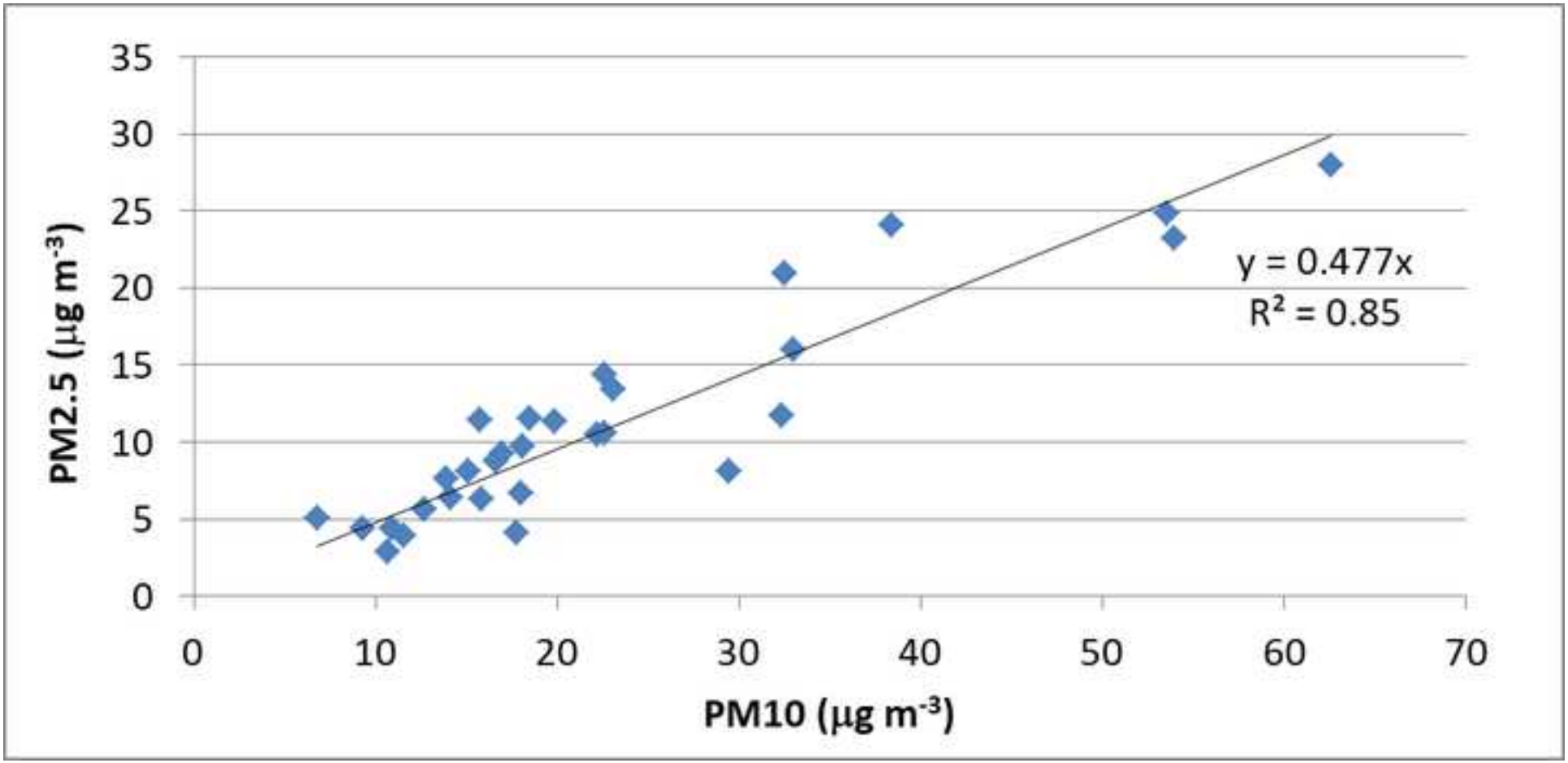

Figure

Click here to download Figure Fig 2.tiff

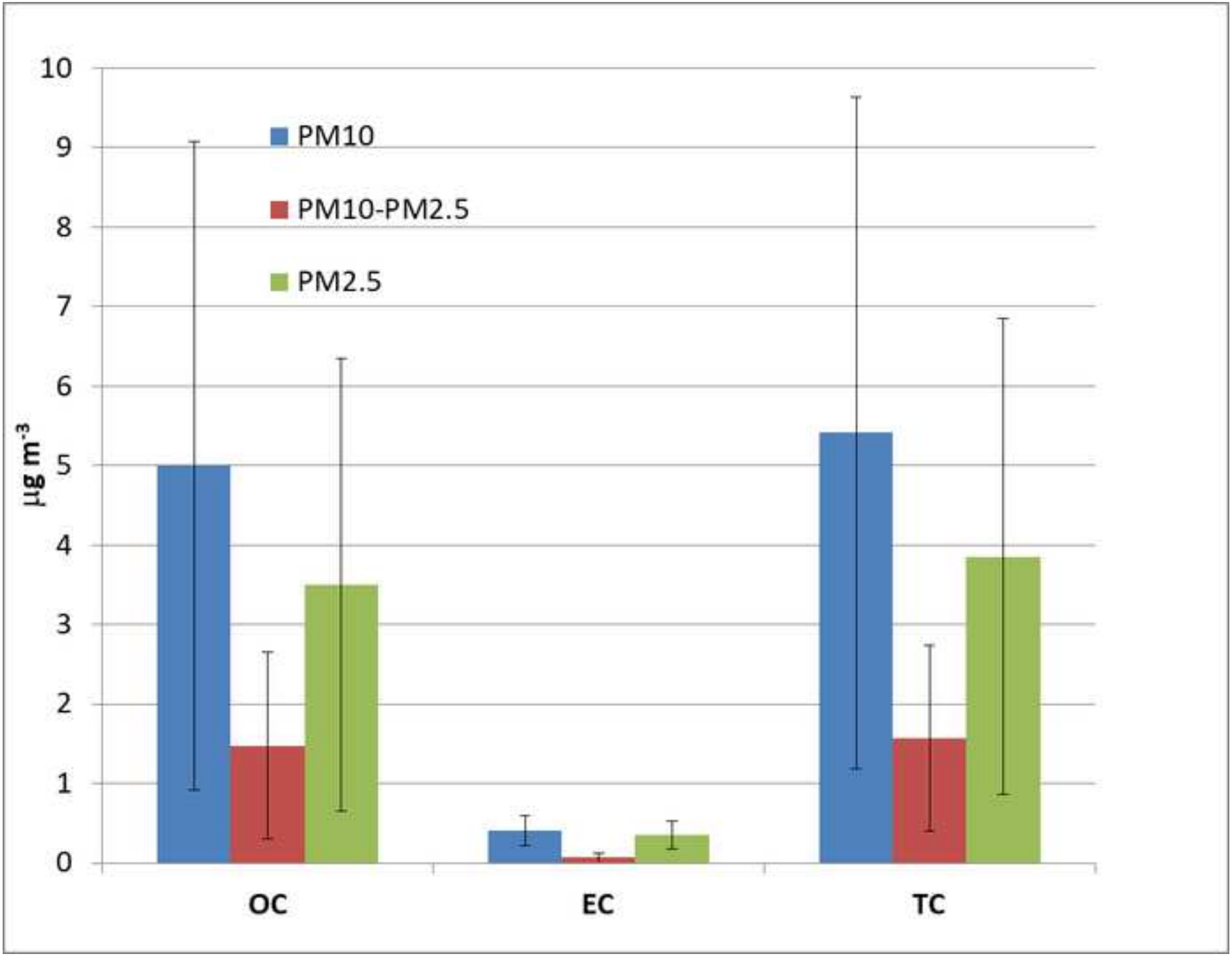

Figure

Click here to download Figure Fig 3.tiff

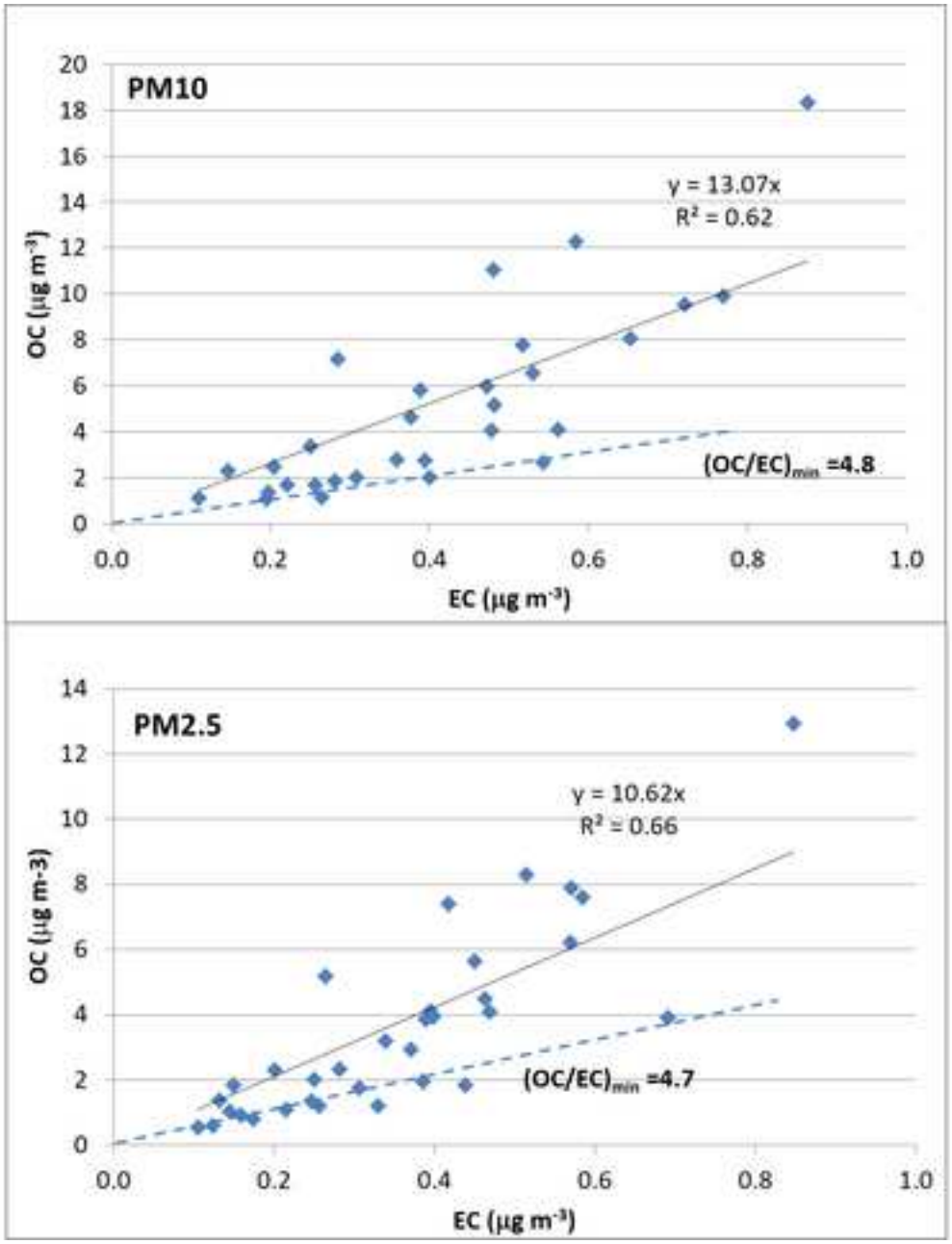

Figure

Click here to download Figure Fig 4.tiff

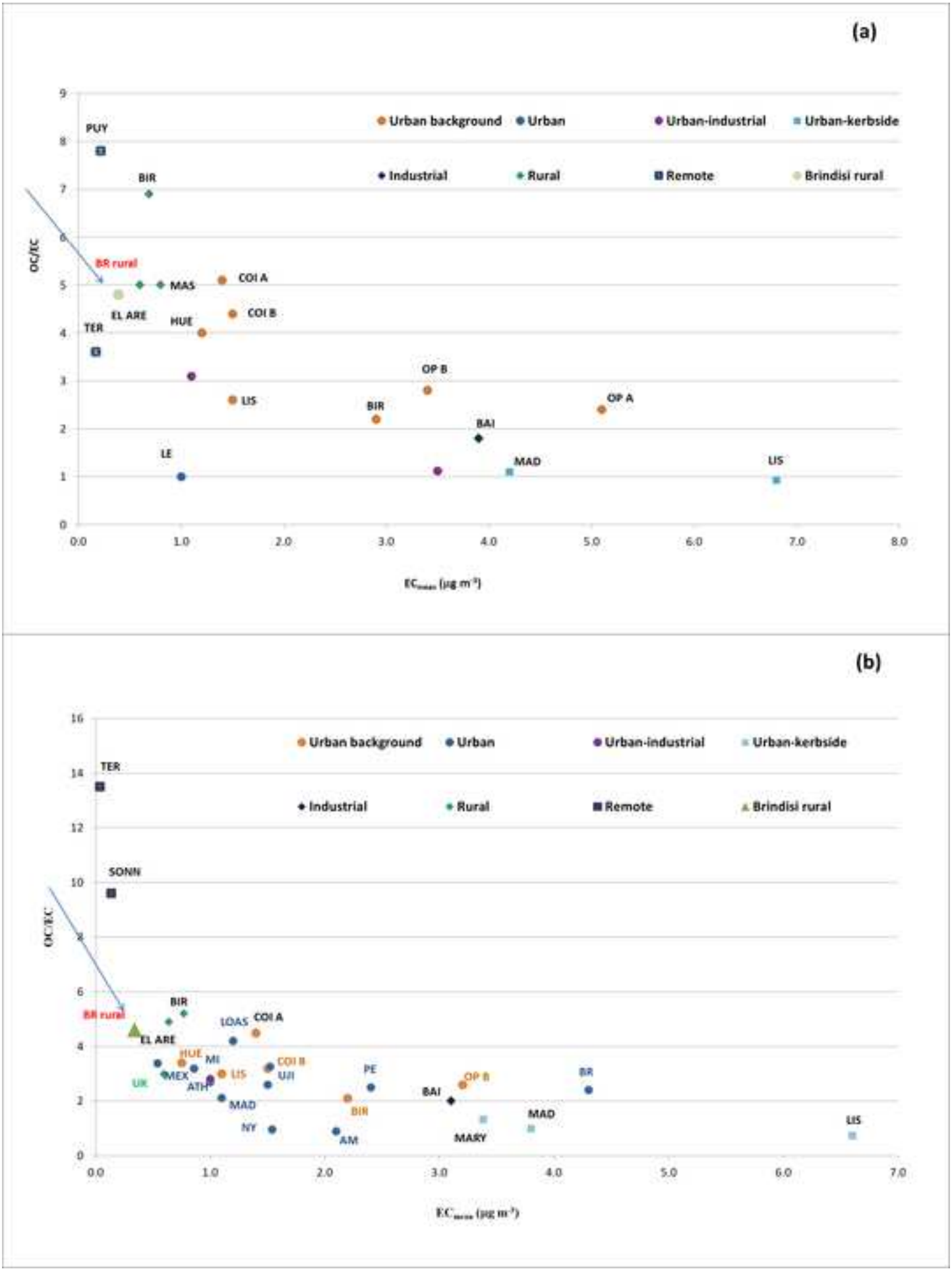

Figure

Click here to download Figure Fig 5.tiff

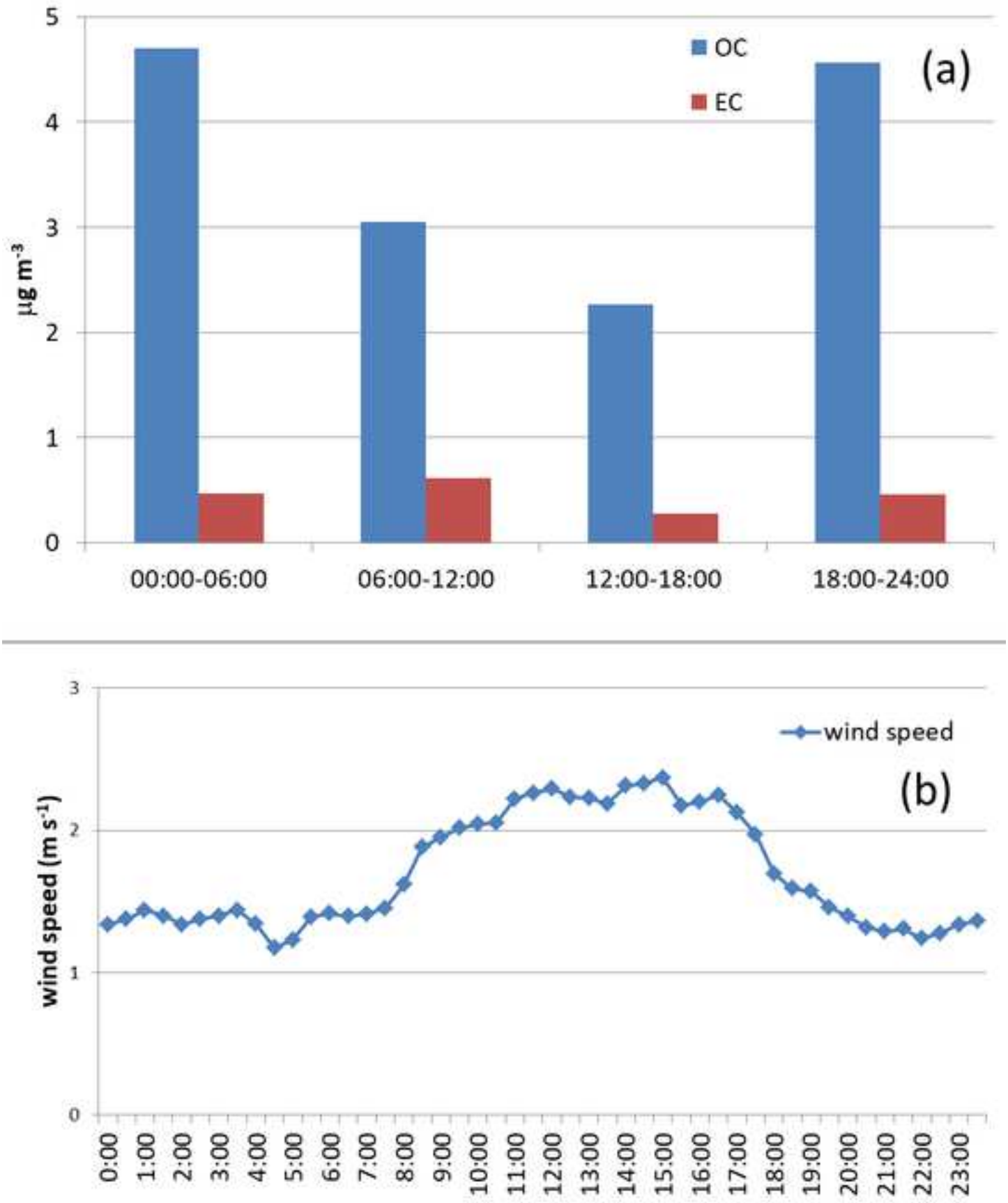

Figure

Click here to download Figure Fig 6.tiff

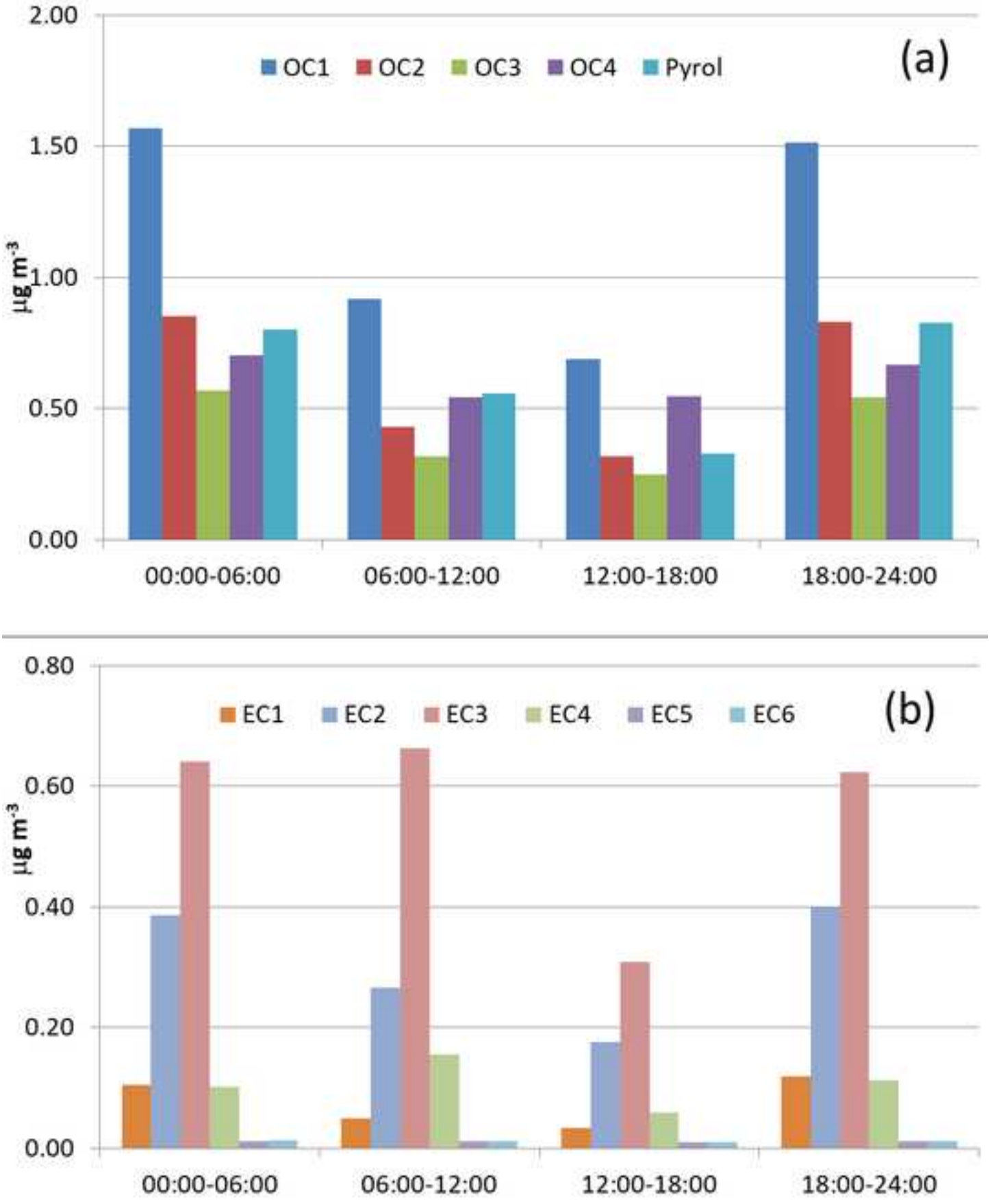

Figure

Click here to download Figure Fig 7.tif

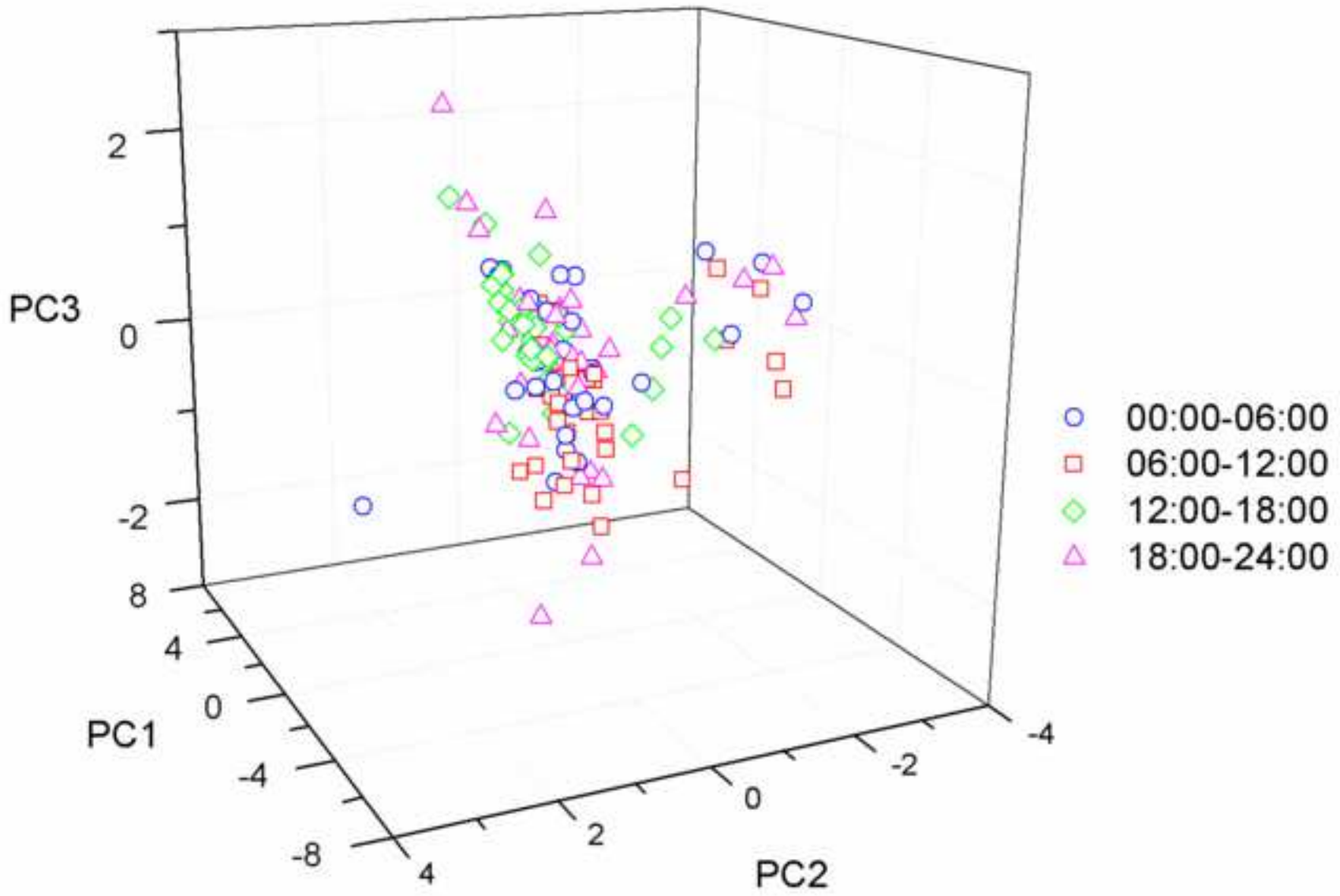

Figure

Click here to download Figure Fig 8.tiff

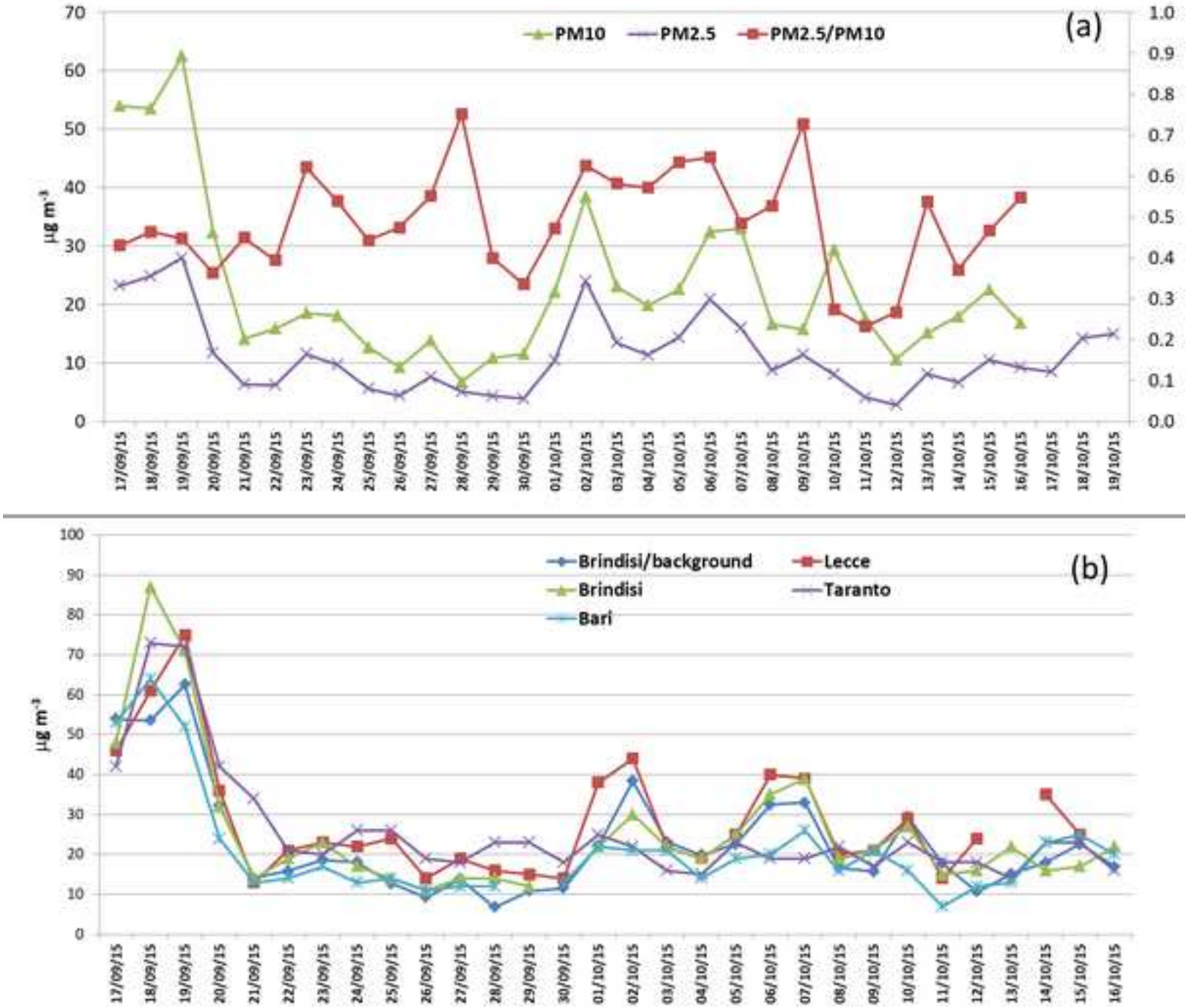

Figure

Click here to download Figure Fig 9.tiff

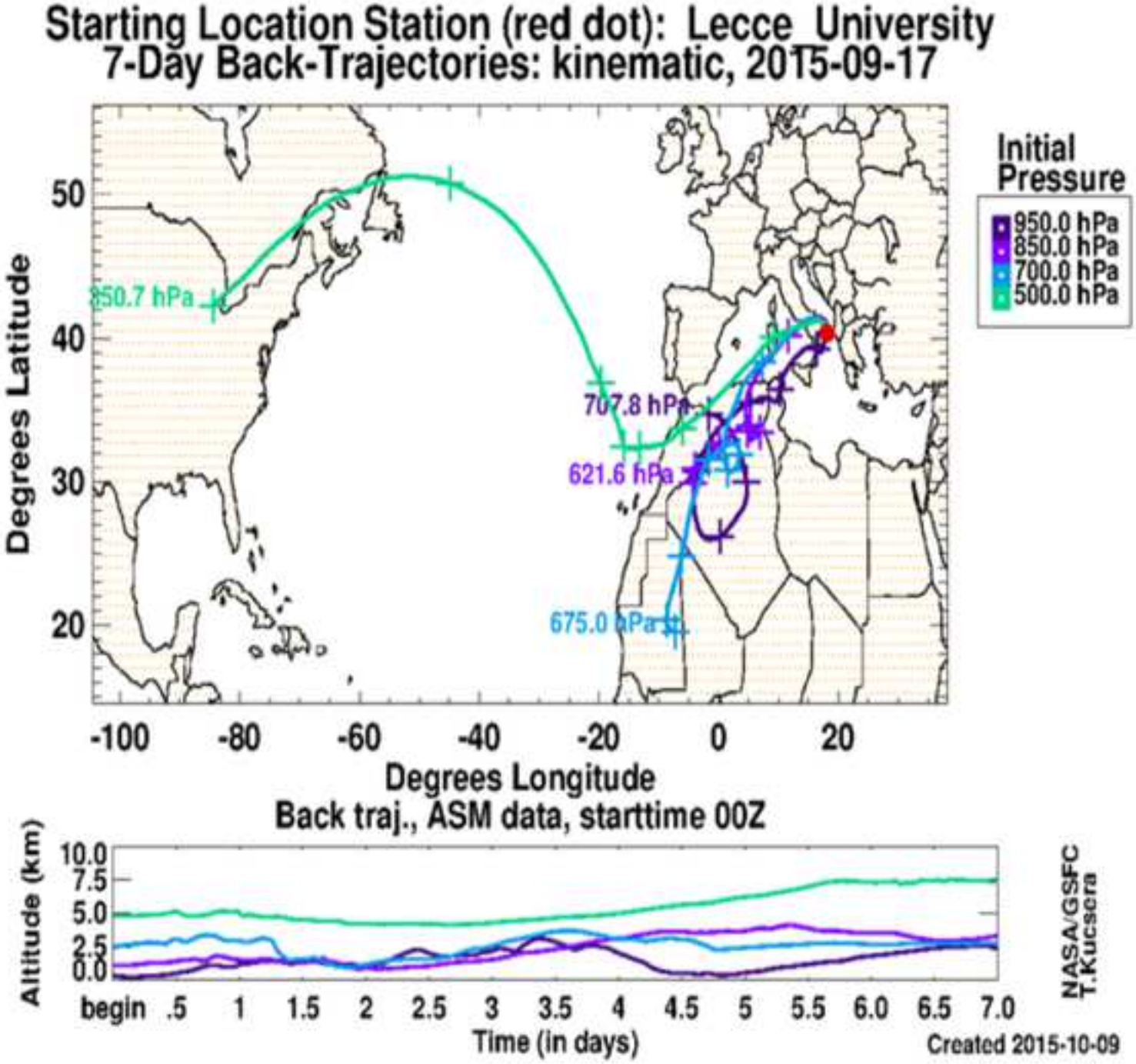

Figure

Click here to download Figure Fig 10.tiff

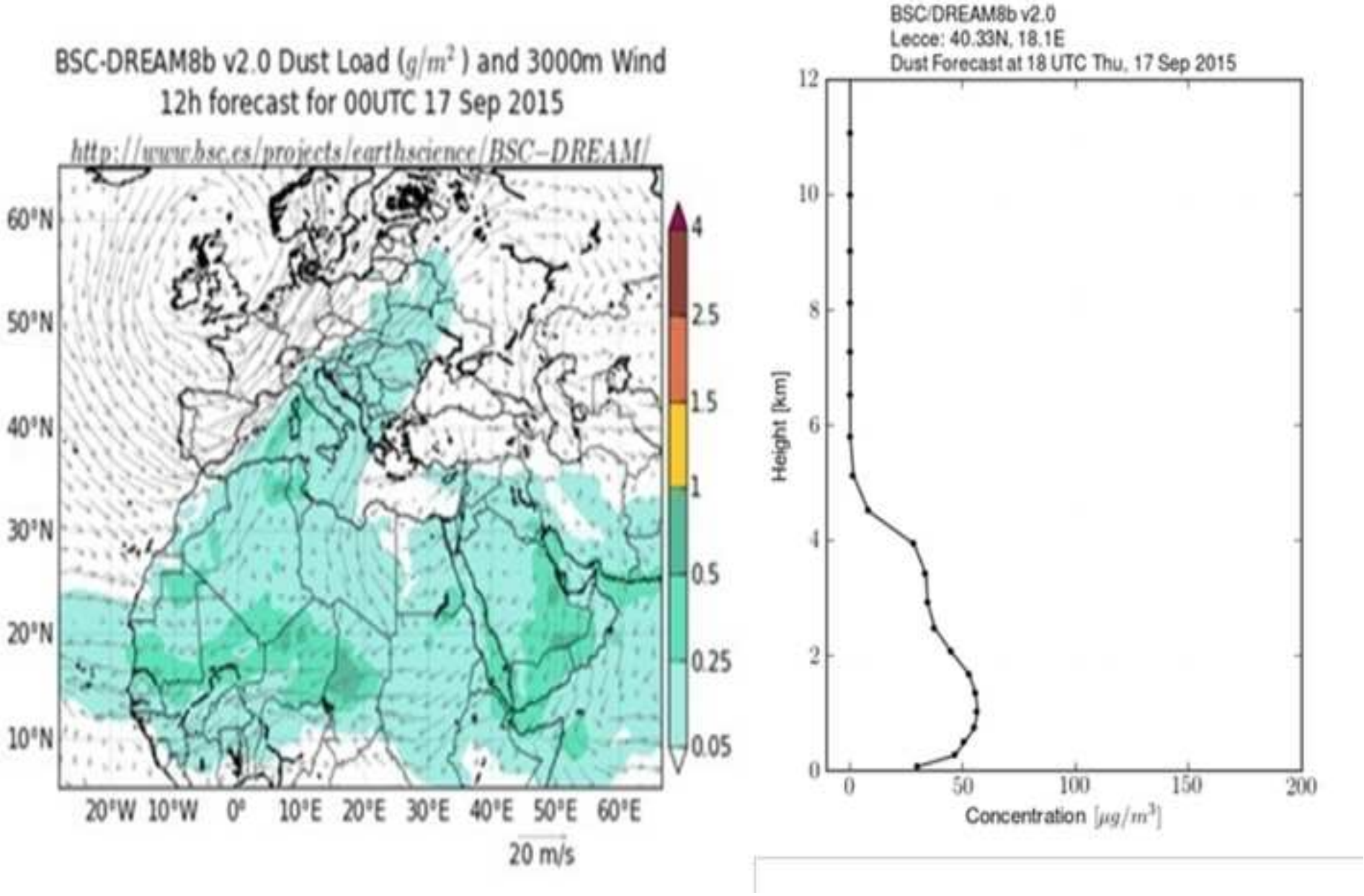

Figure

Click here to download Figure Fig 11.tiff

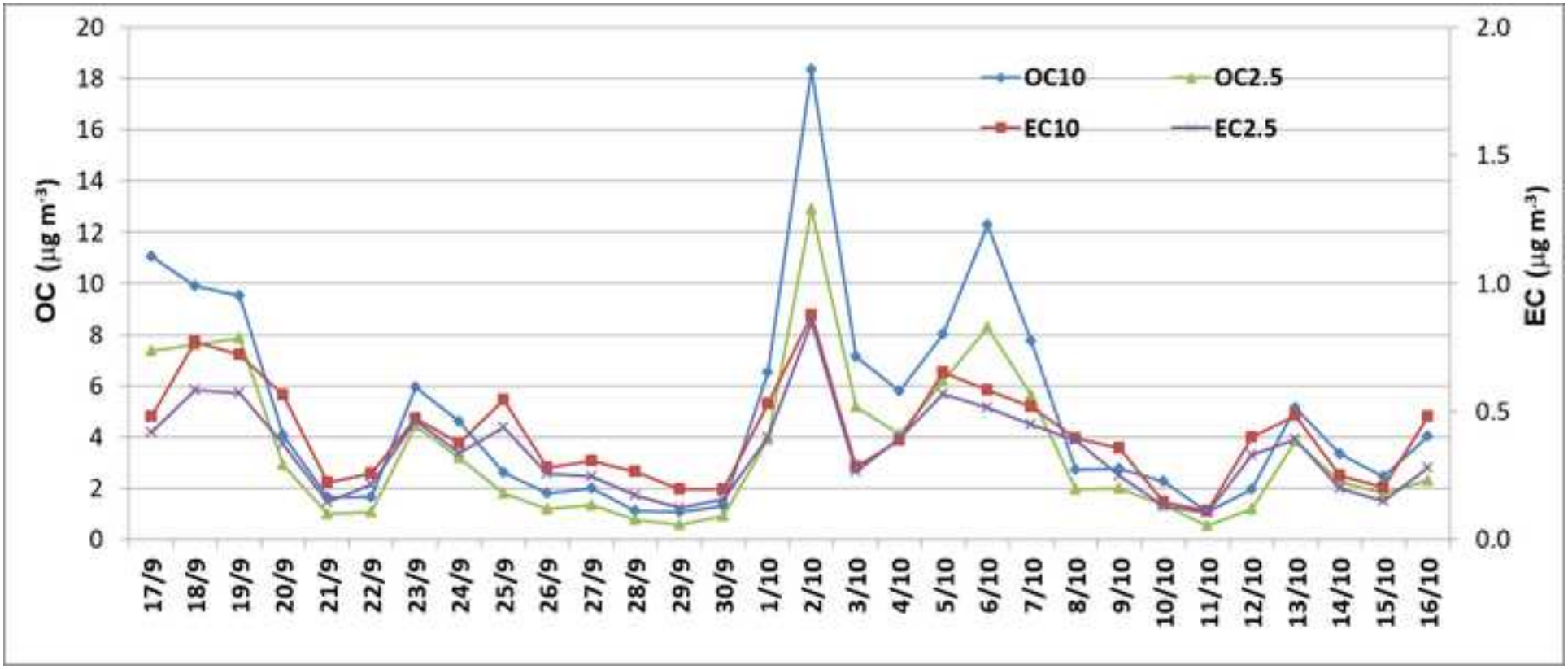

Figure

Click here to download Figure Fig 12.tiff

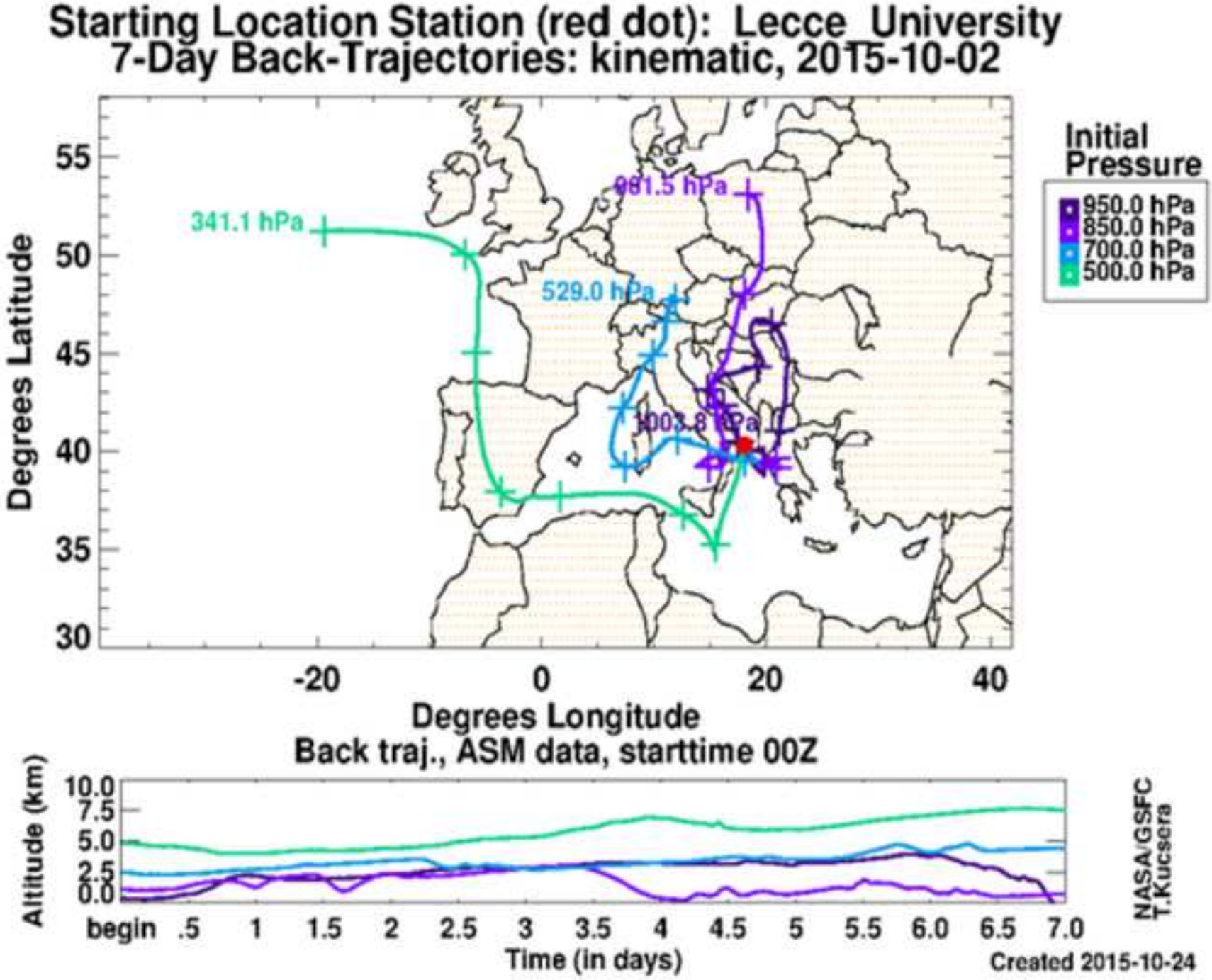

Figure

Click here to download Figure Fig 13.tif

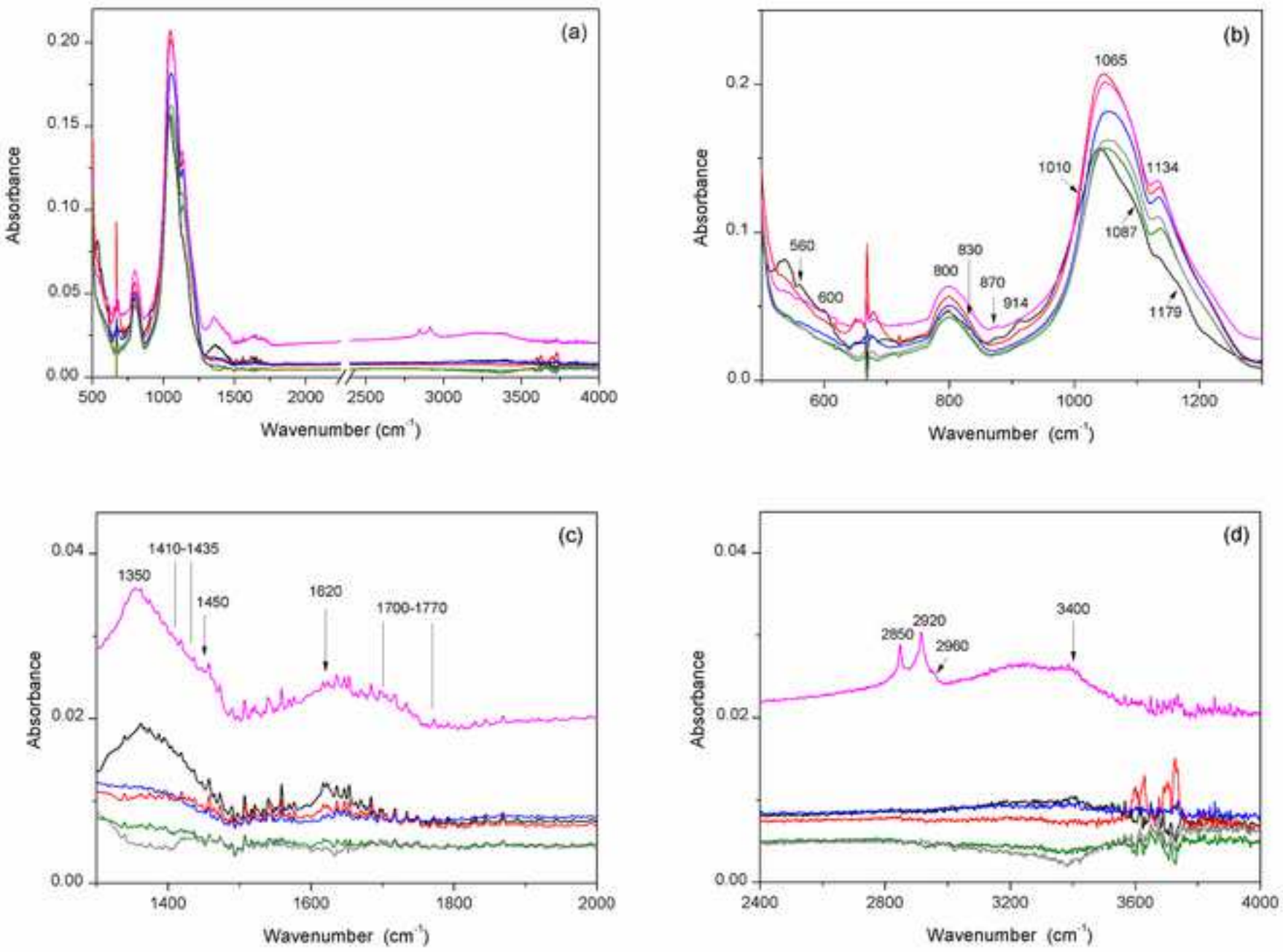

Table 1 Summary statistics for PM10 and PM2.5 sampled for 24h at Brindisi rural site

	OC ($\mu g\ m^{-3}$)	EC ($\mu g\ m^{-3}$)	TC ($\mu g\ m^{-3}$)	TCA ($\mu g\ m^{-3}$)	PM ($\mu g\ m^{-3}$)	OC_{sec} ($\mu g\ m^{-3}$)	OC_{prim} ($\mu g\ m^{-3}$)	OC/EC ($\mu g\ m^{-3}$)
PM10	5 ± 4	0.41 ± 0.19	5.4 ± 4.2	7 ± 6	23 ± 14	3 ± 3	2.0 ± 0.9	11 ± 4
PM2.5	3.5 ± 2.8	0.35 ± 0.18	4 ± 3	5 ± 4	11 ± 6	1.9 ± 2.2	1.6 ± 0.8	9 ± 4

Table 2 Correlation matrix between carbonaceous particulate matter and meteorological parameters. a) PM10; b) PM2.5 24 hours; c) PM2.5 6 hours

	LogOC	*LogEC*	*$LogOC_{sec}$*	*$LogOC_{prim}$*	*vv*	*T*
a) PM10						
LogOC	1					
LogEC	**0,81**	1				
$LogOC_{sec}$	**0,82**	**0,44**	1			
$LogOC_{prim}$	**0,81**	**1,00**	**0,44**	1		
vv	**-0,70**	**-0,77**	**-0,42**	**-0,77**	1	
T	**0,52**	0,39	**0,47**	0,39	-0,23	1
b) PM2.5						
LogOC	1					
LogEC	**0,86**	1				
$LogOC_{sec}$	**0,87**	**0,57**	1			
$LogOC_{prim}$	**0,86**	**1,00**	**0,57**	1		
vv	**-0,68**	**-0,83**	**-0,42**	**-0,83**	1	
T	**0,49**	0,28	**0,47**	0,28	-0,13	1
c) PM2.5 6 hours						
LogOC	1					
LogEC	**0,80**	1				
$LogOC_{sec}$	**0,79**	0,33	1			
$LogOC_{prim}$	**0,80**	1,00	0,33	1		
vv	**-0,74**	**-0,72**	**-0,45**	**-0,72**	1	
T	**0,58**	0,24	**0,46**	0,24	0,10	1

Table 3 Factor loadings of the original variables OC1, OC2, OC3, OC4, Pyrol, EC1, EC2, EC3 and EC4

	PC1	PC2	PC3
OC4	-0.527	0.841	-0.097
OC1	-0.964	0.041	0.070
OC2	-0.929	0.015	0.020
OC3	-0.948	-0.004	0.020
Pyrol	-0.968	-0.096	0.000
EC1	-0.799	-0.053	0.512
EC2	-0.976	-0.085	0.053
EC3	-0.957	-0.139	-0.103
EC4	-0.783	-0.180	-0.531

Table 4 Functional groups and their observed ATR-FTIR spectral frequencies

Functional groups	IR Frequency cm^{-1}
Aliphatic saturated C-C-H	1450, 2800-3000
Aliphatic unsaturated C=C-H	2900-3100
Aromatic C=C-H	3000-3100
Non-acid carbonyl C=O	1640-1850
Carboxylic acid COOH	1640-1850
Alcohol C-OH	3100-3500
Water	3100-3500, 1640
Amine NH_2	3400, 1625
Carbonate	880, 1410-1435
Sulfate	600-50, 1110-1090
SiO_2, silicate	1065, 800
Ammonium NH_4^+	1420, 3040, 3230
Nitrate	815-40, 1350-1380
hydrogen sulfate	563, 850, 1087, 1180